Modelling charge transport in high-mobility molecular semiconductors: balancing electronic structure and quantum dynamics methods with the help of experiments

Tahereh Nematiaram, Alessandro Troisi*

Dept. of Chemistry and Materials Innovation Factory, University of Liverpool, Liverpool L69 7ZD, U.K.

a.troisi@liverpool.ac.uk

Abstract

Computing the charge mobility of molecular semiconductors requires a balanced set of approximations covering both the electronic structure of the Hamiltonian parameters and the modelling of the charge dynamics. For problems of such complexity, it is hard to make progress without validating independently each layer of approximation. In this perspective paper, we survey how all terms of the model Hamiltonian can be computed and validated by independent experiments and discuss whether some common approximations made to build the model Hamiltonian are valid. We then consider the range of quantum dynamics approaches used to model the charge carrier dynamics stressing the strong and weak points of each method on the basis of the available computational results. Finally, we discuss non-trivial aspects and novel opportunities related to the comparison of theoretical predictions with recent experimental data.

1. Introduction

Molecular semiconductors have been one of the most consistently investigated topics in chemistry and physics across the past few decades.[1–6] The early fundamental studies on charge transport[7,8] or excited states[9] were only speculatively linked to potential applications in electronics. The situation changed rapidly in the early 2000s due to critical advances in the fabrication of organic electronic devices that enabled the reproducible measurements of intrinsic charge mobilities in single-crystal devices for a range of molecules in thin-film transistor configurations.[10,11] These experiments had a major impact on the development of technology based organic thin-film transistors[6] and became one of the pillars of modern organic electronics.[12] The same experiments had a fairly unanticipated effect on the theory of molecular semiconductors that, by that time, seemed fairly established. It became immediately clear that the measured charge mobility of high purity crystals of the order of 1 cm^2/Vs was too high to be fully consistent with a simple charge hopping mechanism and too low to be fully consistent with a band transport mechanism.[13] While many early theories dealing with the transition regime between hopping and band transport existed,[14] an additional complication soon became evident for molecular semiconductors. The thermal motion of molecules at room temperature is sufficient to cause a fluctuation of the transfer integrals between neighboring molecules of amplitude comparable to that of the average transfer integral.[15] This dynamic disorder appeared to be one of the limiting factors to charge mobility,[16]

a specific feature of molecular semiconductors. It originates from the softness of the inter-molecular interactions and the sensitivity of the transfer integral to the small relative displacements of the molecules, a fact, the latter, that has been rediscovered many times in the chemical literature.[17–19]

The problem of predicting the charge mobility in molecular semiconductors has since then remained in the spotlight of chemical physics because it combines all the desirable elements of benchmark theoretical problems: (i) continuous experimental interests fueled by potential applications, (ii) easy formulation of the problem, and (iii) failure of the traditional approaches. In essence, the problem consists in the prediction of the quantum dynamics in a system with strong coupling between electronic and nuclear degrees of freedom where it is not easy to introduce the standard approximations because all the relevant time/energy scales coincide. It is therefore not surprising that virtually all the tools of quantum dynamics simulations have been considered for this problem and a review of the proposed methodologies maps very well into the broad set of quantum simulation methods currently in use.

With the proliferation of the theoretical approaches and experimental mobility data to compare with, a different problem soon became apparent. Most transport models, even when based on opposite assumptions, could reproduce the experimental data with a suitable choice of parameters. To avoid this situation, electronic structure calculations of the realistic parameters for the system under study are coupled with a theory of charge transport producing theoretical mobility to be compared with the experimental one without an adjustable parameter. All works that compare computed and experimental mobility are necessarily based on three separate sets of approximations: (i) those required by the electronic structure calculation, (ii) those needed to extract the parameters for the mobility calculations, and (iii) those included in the approximated quantum dynamics. Very frequently, each team of theoreticians makes different choices for all these approximations and the comparison of the final result against the experiment (itself subject to non-negligible uncertainly) does not help identifying the best choices and making rapid progress.

The goal of this perspective is to unpick the many layers of approximation present (and sometimes hidden) in the computation of the mobility and evaluate such approximations independently rather than from the final computed mobility. More specifically, we first analyze how the specific terms of the Hamiltonian can be computed, how independent experiments can help validating them, and whether some common approximations made to build the model Hamiltonian are valid (Section 2). We then consider separately the range of quantum dynamics approximations used to model the charge carrier dynamics in high mobility materials stressing strong and weak points of each method, often on the basis of the available computational results (Section 3). In Section 4, before the concluding outlook, we highlight some non-

trivial problems and novel opportunities in comparison with experimental data. We tried to keep this work focused within the scope just described and we refer the readers more interested in a comprehensive review of this topic to the excellent articles in refs.[6,20–23].

2. The model Hamiltonian and the computation and validation of its parameters

Model Hamiltonian. The starting point for all the methods developed for evaluating charge transport in the intermediate regime is the following Hamiltonian,

$$\hat{H} = \sum_i \varepsilon_i \hat{c}_i^+ \hat{c}_i + \sum_{<ij>} J_{ij}^0 \hat{c}_i^+ \hat{c}_j + \sum_M \hbar\omega_M (\hat{a}_M^+ \hat{a}_M + \frac{1}{2}) + \sum_{i,M} g_{i,M} \frac{1}{\sqrt{2}} (\hat{a}_M^+ + \hat{a}_M) \hat{c}_i^+ \hat{c}_i + \sum_{i \neq j,M} g_{ij,M} \frac{1}{\sqrt{2}} (\hat{a}_M^+ + \hat{a}_M) \hat{c}_i^+ \hat{c}_j \quad (1)$$

where the first two terms denote the electronic part of the Hamiltonian, the third term stands for the lattice phonons, and the last two terms are associated with local and nonlocal electron-phonon couplings; ε_i represents the on-site electronic energy of the hole; J_{ij}^0 are the transfer integral elements between adjacent molecules at the equilibrium geometry; $\hat{c}_i^+ (\hat{c}_i)$ are the creation (annihilation) operator for a hole at site *i* (there is one state per site); <*ij*> nearest-neighbor pairs of occupied sites; $\hbar$ is the reduced Planck constant; ω_M is the phonon frequency of mode *M*; $g_{i,M}$ and $g_{ij,M}$ are the local and nonlocal electron-phonon couplings measuring the strength of interaction between charge carriers and intra-molecular and inter-molecular vibrations; $\hat{a}_M^+ (\hat{a}_M)$ are the phonon creation (annihilation) operators. What makes the study of high-mobility molecular semiconductors challenging is the fact that the Hamiltonian parameters, i.e. electronic coupling between the molecules *J* often in the interval [10 - 200] meV, vibrational energies in the range of [5 - 200] meV, local electron-phonon coupling (reorganization energy) in the interval [20 - 500] meV, nonlocal electron-phonon coupling (dynamic disorder) in the range of [10 - 100] meV, and thermal energy at room temperature (k_BT ~ 25 meV) generally differ by not more than an order of magnitude meaning that most approximations relying on energy scale separation cannot be applied. In the remainder of this section, we outline the computational methods used to evaluate the Hamiltonian parameters from first principle and their validation. Equation (1) also implies a linear coupling between fermions and phonons and the validity of the harmonic approximation for the phonons. Below we also discuss the validity of both approximations alongside methods that do not rely on them.

Transfer integrals. A variety of methods such as Kohn-Sham equation based approaches,[24–27] density functional theory,[18,28–32] pseudopotentials,[33–35] and localized orbital methods[36] are developed to compute the transfer integrals *J*. The difference between computed transfer integrals within different methods can be very small (e.g. less than 15%) as reported for rubrene,[37,38] pentacene,[39,40] for ~70% and ~80% of the samples studied respectively in Ref.[41] and Ref.[42], although there are counterexamples where the difference can be larger.[41,43,44] It is also important to note that the band-structure calculations obtained from DFT-based methods are not very sensitive to the size of the basis set with small basis sets already providing quantitatively correct results.[45] A summary of available methods for computing the transfer integrals can be found e.g. in Refs.[5,46,47] with a critical investigation of the methods' speed and accuracy provided in Ref.[48]. Computed band structures can be validated for example by angle-resolved photoemission experiments (ARPES) of crystalline organic semiconductors,[49–51] and the level of agreement supports a very high degree of confidence in the evaluation of this component of the Hamiltonian. It is repeatedly mentioned that the eq. (1) is valid for narrow-band semiconductors. The validity of this assumption can be easily verified by considering the set of 40,000 molecular semiconductors extracted from the Cambridge Structural Database (CSD),[52] as identified in a recent work from our group.[53] The results indicate that the median energy separation between HOMO and HOMO-1 energy levels is 0.66 eV. We found that in this dataset the largest transfer integral is never greater than 0.4 eV (with the median being 0.14 eV).[54] Therefore, one can conclude that the band energies do not overlap effectively and the approximation that the valence band originates from the HOMO orbital is broadly valid, with the obvious exception of molecules with degenerate HOMO and HOMO-1 (~0.08% of the sample considered).

Phonon calculations. An accurate calculation of *high-frequency* vibrational modes of organic semiconductors is easily achievable based on routine DFT methods. Most of the theoretical studies compute the phonons of an isolated single molecule (rather than on a periodic crystal) and utilize it to interpret the crystal phonons.[55,56] This approach is valid because, when the full phonon band is computed,[57–59] the high-frequency modes are shown to be essentially dispersion-less, i.e. very localized. There are also other studies that consider a molecule embedded in the shell of neighboring rigid molecules within a nonperiodic Quantum Mechanics/Molecular Mechanics (QM/MM) method[60,61] or with the entire cluster studied quantum mechanically (employing the DFTB method[62]) but keeping the embedding molecules rigid.[63] In essence, the calculations of high-frequency modes are in excellent agreement with each other's and with experimental data obtained from FTIR and Raman spectroscopy.[58,64,65]

In contrast, computational methods for *low-frequency* vibrations have been developed and validated only more recently. Many researchers adopt empirical force fields which can be inaccurate because of not

being parameterized to reproduce low-frequency phonons.[66,67] On the other hand, accurate density functional calculations of molecular crystals vibrations are very demanding in particular in cases dealing with materials containing hundreds of atoms in their unit cell (a common case for organic crystals) and are typically reserved only for benchmark systems.[68,69] In addition, they are very sensitive to DFT level and, specifically, to the dispersion correction,[70] which is introduced differently in various methods.[58,71]
Specialized Raman spectroscopy setup[61,64] or terahertz(THZ) time-domain spectroscopy[72] are commonly used for extracting information on low-energy phonons. These measurements provide gamma phonon energy which can be used to partially validate the computed phonon spectra[61,72] but do not allow the validation of the acoustic phonons dispersion, which is expected to be important for transport.[59,73,74] Information on the large amplitude (mostly acoustic) modes is provided by the diffuse electron scattering methods,[75,76] which are based on the analysis of electron diffraction pattern: they are useful to quantify the displacement from the equilibrium position but do not give the frequency dependent information required for charge transport models.[76] Recent high-resolution inelastic neutron scattering (INS) measurements on molecular crystals, which give access to the low-energy phonons without being subject to the afore-mentioned constraints, have enabled the validation of low-frequency phonon calculations with great accuracy.[69,72] For example, calculations using plane-wave density functional theory employing the Vienna Ab initio Software Package (VASP)[77] with projector augmented-wave pseudopotentials[78] and the optPBE van der Waals density functional method,[79] proved able to reproduce the INS spectra across all frequency range.[69] Overall, state-of-the-art methods are capable of evaluating phonon modes of molecular crystals with the drawback that the most reliable methods are extremely expensive because of the large unit cell of molecular crystals. These methods are suitable for validating the more approximated strategies described above.
In principle, the full phonon dispersion curve could be obtained from inelastic neutron scattering techniques but the method is extremely challenging, as it requires single crystals, which are hard to grow. Moreover, it is important to have crystals composed of deuterated molecules as they lead to higher coherent and lower incoherent scattering cross-sections for neutrons.[80,81] To the best of our knowledge, experimental phonon band structure data are available only for very few organic crystals of small molecules like naphthalene or anthracene.[82,83]

Local electron phonon couplings. The reorganization energy λ is a global measure of the local-electron phonon coupling that can be defined as,

$$\lambda = E(Q_0) - E(Q) + E(Q) - E(Q_0) \quad (2)$$

where E and E^{+} represent the energy of neutral and charged molecules. These energies are computed at two different geometries indicated by Q and Q^{+} referring respectively to the optimized geometry of the neutral and charged states.[84,85] It is normally computed for isolated molecules in vacuum as several studies have found the effect of the environment to be negligible.[86,87] If the potential energies of neutral and charged state are harmonic and the coupling with the phonons is linear (as implied in eq. 1), the reorganization energy can be decomposed as a sum of contributions over the normal modes and related to the electron-phonon coupling terms as,

$$\lambda = \sum_M \lambda_M = \sum_M \frac{|g_M|^2}{\hbar \omega_M} \tag{3}$$

In this limit each contribution to the reorganization energy λ_M can be computed as,

$$\lambda_M = \frac{1}{2} \hbar \omega_M \Delta Q_M^2 \tag{4}$$

where ΔQ_M represents the displacement along the normal mode *M* between the equilibrium geometries of the neutral and charged molecules.[88–90] Comparing the reorganization energy computed from the four points formula (eq. (2)) or from the normal modes projection method (eqs. (3) and (4)) provides an indication of the validity of the harmonic approximation and the linearity of the local electron-phonon coupling. To investigate the level of correlation between the results of the two methods, we have calculated the reorganization energies from both methods for a set of 500 molecular semiconductors extracted from the CSD[53] (all the calculations are performed at B3LYP/3-21G* level of the theory as implemented in Gaussian 16[91]). As shown in Figure (1), the similarity between the results obtained via the two methods indicates that a linear local electron-phonon coupling and the harmonic approximation are essentially valid approximations.

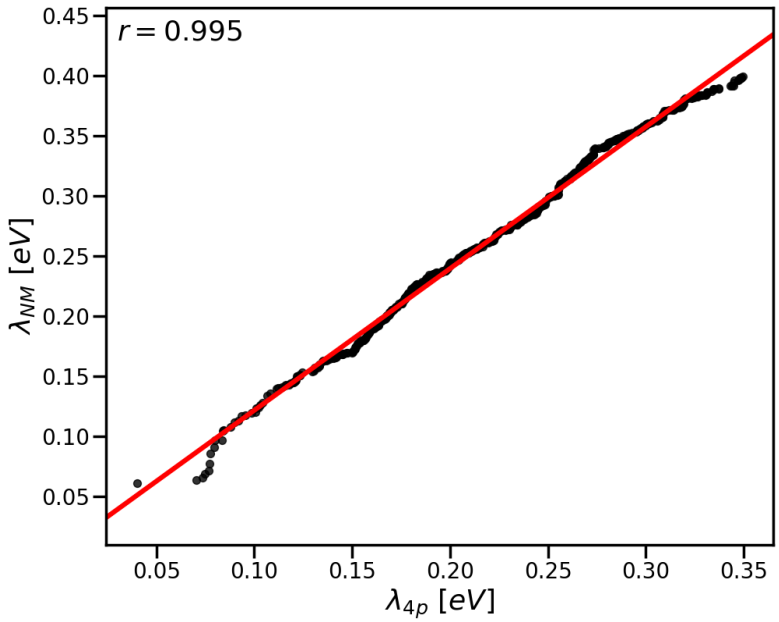

Figure 1. Comparison between the values of reorganization energy obtained based on the adiabatic potential energy surfaces method (4p) and the normal mode (NM) projection at the B3LYP/3-21G* level of the theory.

In literature, it is often stressed that the local electron-phonon couplings are dominated by high-frequency modes in the 900-1600 cm^{-1} range.[92] To validate this statement more quantitatively we analyzed the local electron-phonon coupling and frequencies of a set of 5,000 molecular semiconductors extracted from the CSD.[54] Figure 2 illustrates the spectral density – defined as $B(\omega) = \sum_M \lambda_M \delta(\omega - \omega_M)$ – for this global set. In the numerical analysis, the Dirac delta function is replaced by a Gaussian distribution with standard deviation of 5 cm^{-1}. One can observe that there is a non-negligible contribution to the reorganization energy from low-frequency modes. Considering for each molecule in the dataset the fraction of the reorganization energy originating from high-energy modes (defined as such that $\hbar\omega > 2k_B T$), we find that the median of high-energy modes contribution to the reorganization energy is 84%. This broad range of phonon energies contributing to the local electron-phonon coupling is usually neglected in developing theoretical models for charge transport. For example, semiclassical quantum dynamics methods assume that all the nuclear modes are classical[23] whereas renormalization theories are accurate only in the limit of high-frequency (quantum) phonons.[7,93]

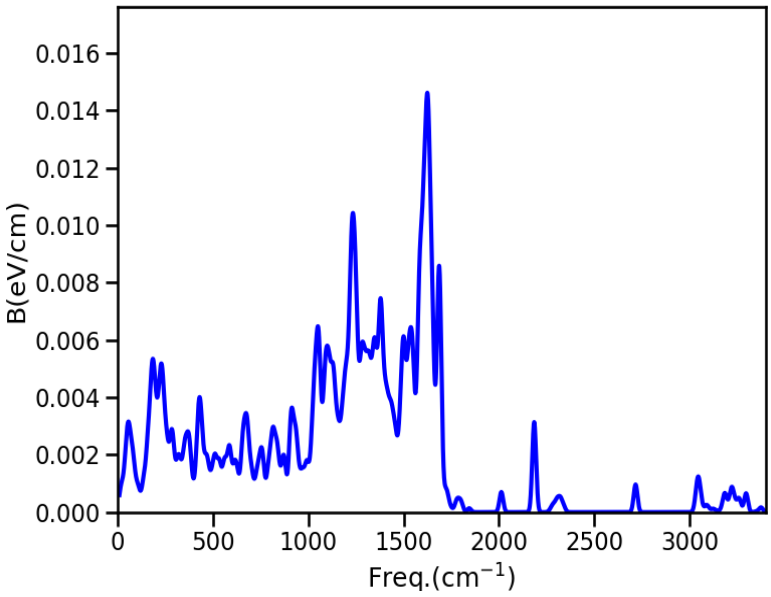

Figure 2. The averaged spectral density *B* for local electron-phonon coupling considering a database of 5k molecular semiconductors extracted from the CSD.

From the experimental point of view, the electron-phonon coupling is directly accessible via high resolution ultraviolet photoelectron spectroscopy (UPS) spectra of gas-phase molecules.[94,95] Malagoli and collaborators have shown that there is a remarkable agreement between the computed reorganization energies on a series of oligoacene molecules and the results of experimental studies utilizing the UPS spectra.[89]

Nonlocal electron-phonon coupling. The nonlocal electron-phonon couplings ($g_{ij,M}$) are generally less investigated than their local counterparts,[96] as they rely on two computationally intensive tasks requiring the transfer integrals' derivative and the phonons calculations.[57,59,63] In the presence of nonlocal electron-phonon coupling, the transfer integral between two electronic states denoted by *i* and *j* in the linear approximation can be written as,

$$J_{ij} = J_{ij}^{0} + \sum_{M} g_{ij,M} Q_M \qquad (5)$$

where J_{ij} indicates the modulated transfer integral. Q_M denotes dimensionless coordinate of the associated normal mode.[57] Therefore, the nonlocal electron-phonon coupling for a given molecular pair *ij* due to mode *M* is,

$$g_{ij,M} = \frac{\partial J_{ij}}{\partial Q_M} \qquad (6)$$

where the Cartesian gradient of the transfer integrals can be computed as,

$$\vec{\nabla} J_{ij} = \{\frac{\partial J_{ij}}{\partial x_k}\} \tag{7}$$

The modes can also be represented as a vector of Cartesian displacements $\vec{Q}_M^C = \{x_k^M\}$ and consequently the nonlocal electron-phonon coupling can be computed as,

$$\vec{g}_{ij,M} = \vec{\nabla} J_{ij} . Q_M^C \tag{8}$$

This coupling gives access to the nonlocal dynamic disorder $\vec{S}_{ij}$, a global measure of the fluctuations of the transfer integrals J_{ij},[57]

$$\sigma_{ij}^2 = \left\langle (J_{ij} - \left\langle J_{ij} \right\rangle)^2 \right\rangle = \sum_M \frac{\left| g_{ij,M} \right|^2}{2} \coth\left(\frac{\hbar \omega_M}{2 k_B T} \right) \tag{9}$$

Because of their computational cost, nonlocal electron-phonon couplings and $\vec{S}_{ij}$ have been evaluated only for a limited number of molecules[24,59,68,97] and there is no direct experimental counterpart to validate the theoretical results. As one can see from eq. 8 their accuracy depends on the accuracy of the transfer integral and the normal modes for which independent experimental validation is possible.

While it is desirable to have materials with small dynamic disorder $\vec{S}_{ij}$, this quantity depends on the electronic and vibrational structure of the materials in such a complex way that it may seem impossible to develop an intuitive understanding of why some materials have smaller or larger dynamic disorder. A recent analysis of 12 materials has suggested that the magnitude of $\vec{S}_{ij}$ is largely dependent on the magnitude of $|\vec{\nabla} J|$ (see Figure 3).[63] One practical implication of this observation is that one can attempt the design of materials with small electron phonon coupling by focusing on the identification of materials with small $|\vec{\nabla} J|$, neglecting the phonon calculations in the first instance or employing more approximated methods for the calculation of the phonons.

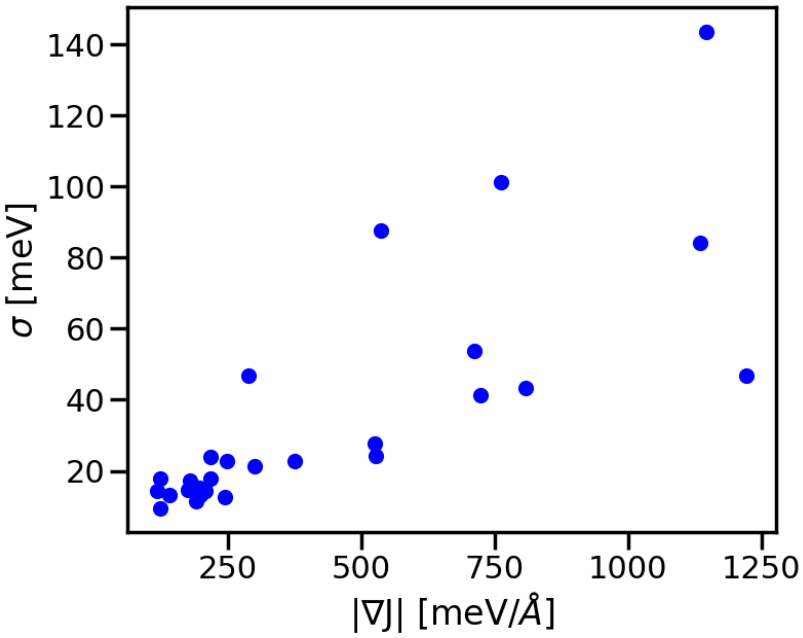

Figure 3. The correlation between dynamic disorder σ and gradient of the transfer integral $|\nabla J|$ for 12 materials. Figure adapted from Ref.[63].

In eqs. (1) and (5) it is assumed that the nonlocal electron-phonon coupling is linear, an assumption more likely to fail for low-frequency modes (more an-harmonic and characterized by larger amplitudes). Because of these concerns, the early evaluations of dynamic disorder employed classical Molecular Dynamics to study the fluctuation of the transfer integral in the time domain, ignoring the decomposition into normal modes and implicitly accounting for non-linearity of electron-phonon coupling and anharmonicity.[15,98,99] The approximation in eqs. (1) and (5) is however extremely convenient especially because parametrization of classical simulations can be very tedious if one wants to consider a large set of chemically different molecules. To check the validity of the linear approximation, we have studied the deviation from linearity for the largest transfer integral of rubrene and 3,6-bis(3-Chlorophenyl)pyrrolo(3,4-c)pyrrole-1,4-dione (identified as "WEBKAP" in the Cambridge Structural Database). The largest transfer integral of these two crystals are of similar magnitude while they present a significantly different dynamic disorder, as such, the transfer integral J (dynamic disorder σ) of WEBKAP and rubrene are respectively 0.146 (0.081) and 0.139 (0.043) eV. The transfer integrals are computed based on the method explained in ref.[18] at the B3LYP/3-21G* level of the theory and the dynamic disorders based on the method developed in ref.[54]. These structurally different materials provide a reasonable starting point for preliminary investigation of linear coupling assumption. In the considered structures, for each mode, the deviation from linearity can be defined as $D_M = |g_M - (J(Q_M = 1) - J^0)| / g_M$ and expressed as a percentage. The median D_M for rubrene and WEBKAP is just 3.6% and 2.8%, respectively; the

distribution of this quantity is shown in Figure 4(a and e) with an illustration of the type of non-linearity that one can expect to find in their right hand side panels (b-d) and (f-h) corresponding to D_M = 0, 5 and 14%.

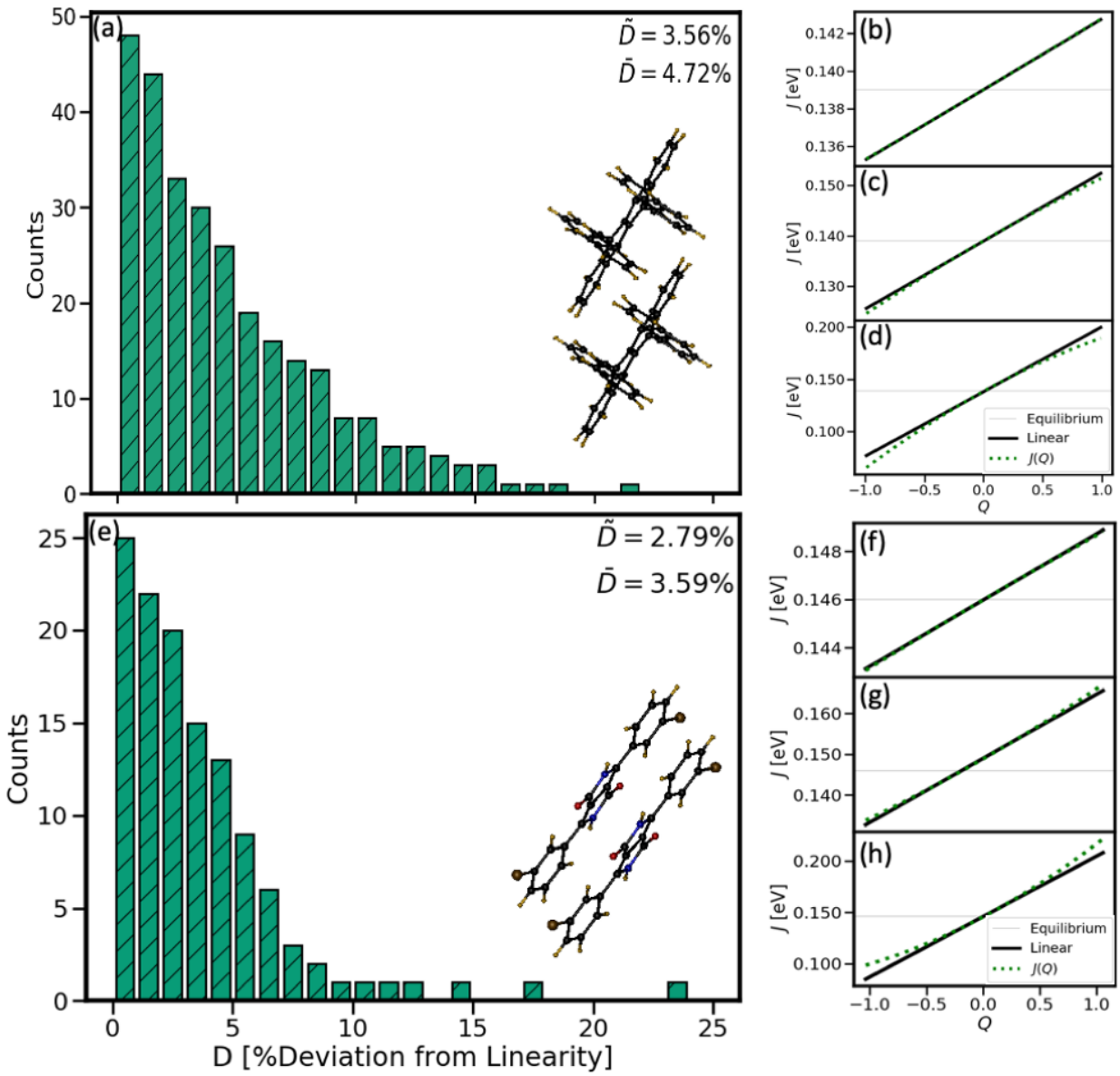

Figure 4. (a) Distribution of deviation from linear electron-phonon coupling approximation for the highest transfer integral of rubrene with the associated molecular pair. (b-d) Comparison between linear approximation and real electron-phonon couplings. The light grey line indicates the transfer integral at equilibrium geometry (in the absence of nonlocal electron-phonon coupling). The corresponding values of deviation from top to bottom are 0, 5 and 14%. The same set of analysis is reported in panels (e-h) for WEBKAP. The small nonlocal electron-phonon couplings ($|g_M|<10^{-5}$ eV) are neglected in our analysis.

These results suggest that considering only a liner nonlocal electron-phonon coupling should be sufficiently accurate at least for the considered structures but more importantly, this analysis

demonstrates that the linearity of the nonlocal electron-phonon coupling can be easily verified. The advantages of the linear approximation are so significant that it is worth resorting to them with additional checks if deemed necessary.

Another common approximation is that all the phonons contributing to nonlocal electron-phonon couplings are classical (i.e. $\hbar\omega \leq k_B T$) and explicit calculations allow a direct validation of this assumption. Indeed, the contribution of high frequency modes to the nonlocal electron-phonon coupling is not completely negligible.[16,59,69] An example of such calculation is shown in Figure (5) for the highest transfer integral of rubrene,[59] where the contribution of high-frequency modes to the fluctuation of the transfer integral at room temperature is 9%. The percentage appears to be small despite strong coupling with high-frequency modes because these modes are not populated at room temperature. The presence of high-frequency modes contributing to the nonlocal electron-phonon coupling is usually neglected in all semiclassical simulation methods.[16,100–102]

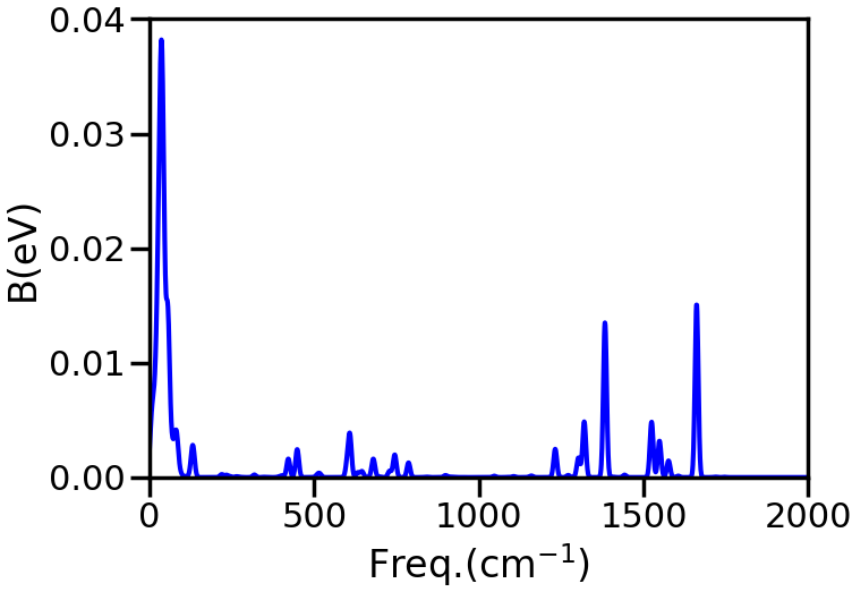

Figure 5. The spectral density $B_{ij}(\omega)=\frac{1}{2\hbar}\sum_M g_{ij,M}^2\delta(\omega-\omega_M)$ for the largest transfer integral of rubrene crystal. Figure adapted from Ref.[59].

3. Models for charge transport

In this section, we give an overview of the various theoretical approaches developed for evaluating charge transport in molecular semiconductors, their theoretical principles, the physical insight provided by each one of them and an estimation of their validity range. The focus of this work is on high-mobility materials

(e.g. μ>0.5 cm^2/Vs) and therefore mechanisms of transport that retain some degree of quantum coherence of the carrier. A totally incoherent mechanism, where the carrier hops from molecule to molecule with a characteristic rate constant, can be ruled out for high-mobility materials on the basis of elementary arguments. Simply observing that incoherent hopping cannot be faster than vibrational relaxation, the maximum mobility that could be described by hopping was estimated in ref.[103] as $\mu_{hop}^{MAX} \sim \frac{2\pi c \tilde{\delta} e L^2}{k_B T}$, where *c* is the speed of light, *L* the shortest distance between the molecules, and $\tilde{\delta}$ the low temperature width in wavenumbers of Raman vibrational peaks in the solid state. Such relation, which only contains experimental parameters, suggests that room temperature mobility exceeding ~0.1 cm^2/Vs cannot be due to a completely incoherent transport mechanism. Incoherent transport models are still important in many interesting cases (very narrow bands, trap-limited transport) and are extremely useful as limiting theories also for high-mobility transport. For this reason, they will be briefly outlined here with more extensive discussion available from other recent reviews.[20,23,38,104]

Incoherent hopping mechanisms. One of the simplest and still widely used approaches for the evaluation of the mobility is based on the calculation of the hopping rate of a charge between neighboring molecules k^{HOP}. For molecules in a perfect crystal, one can use the network of rate constants to evaluate the charge diffusion coefficients analytically[105] or using a Kinetic Monte Carlo scheme[56] (more useful if one wishes to include additional effects of disorder[106,107]). One should instead be wary of expressions of the mobility which appear to be weighted averages of the hopping rates as,[37,108]

$$\mu = \frac{e}{k_B T} \frac{1}{2d} \sum_{n=1}^{N} r_n^2 k_n^{HOP} P_n \qquad (10)$$

where the sum is over all neighboring molecules *N*, with *d* being the spatial dimensionality, *n* a specific hopping pathway with the intermolecular center-to-center distances r_n, and P_n the hopping probability determined as $P_n = k_n^{HOP} \Big/ \sum_{m=1}^{N} k_m^{HOP}$. These contradict the principle that the overall rate of a process is determined by the slower rates (not an average of all rates) and fail when some rate constants are set to zero giving a finite mobility whereas the correct mobility would be zero.

One of the most used expressions of the hopping rate is that proposed by Marcus[109] (or in a slightly different form by Holstein[110]):

$$k^{HOP} = \frac{|J|^2}{\hbar}\left(\frac{\pi}{\lambda k_B T}\right)^{1/2} \exp\left(-\frac{\lambda}{4k_B T}\right) \quad (11)$$

The conditions for the validity of eq. (11) are that: (i) $|J| << \lambda$, (ii) all nuclear modes coupled with the charge transfer can be treated classically, and (iii) the vibrational relaxation is faster than the hopping rate. The violation of the last condition makes the concept of rate constant undefined and makes the transport coherent to some extent, as discussed above. A hopping rate can be still defined for *J* as large as $\sim \lambda/2$ (beyond this value there is no stable state with a charge localized on a molecule) and high-frequency modes. In the simplest case of harmonic one-dimensional potential energy surfaces with frequency *ω* the rate can be expressed as,[111]

$$k^{HOP} = \frac{\omega}{2\pi} k_{LZ} \Gamma \exp\left(-\frac{(\Delta G + \lambda)^2}{4\lambda k_B T}\right) \quad (12)$$

with Δ*G* being the exothermicity of the reaction, Γ the nuclear tunneling factor often taken equal to one as it is expected to be important only in low temperatures and k_{LZ} the thermally averaged Landau-Zener coefficient corresponding to the "electronic tunneling".[112–114] The adiabatic and nonadiabatic (i.e. the Marcus formula) limits are then recovered by $k_{LZ} = 1$ and $k_{LZ} = \frac{2|J|^2}{\hbar\omega}\sqrt{\frac{\pi^3}{\lambda k_B T}}$, respectively.[115,116] The idea of introducing a single effective high-frequency mode[117] was adopted by several authors, for example, to try to reproduce isotopic effects.[118] To include the effect of multiple modes, Landi et al. have utilized second-order cumulant (SOC) expansion of the time-dependent reduced density matrix highlighting the importance of multiple modes to describe the temperature dependence of the rate.[119] Yan et al. have calculated the exact memory kernels of the Nakajima-Zwanzig-Mori GME for a one dimensional Holstein type model by employing the Dyson relation for the exact memory kernel, combined with the hierarchical equations of motion method.[120]

Band transport. Band transport theory relies on the solution of the electronic problem in a perfect unperturbed lattice. According to this theory, the electrons form Bloch waves which can be identified by a well-defined momentum *k* and the energy band dispersion *E*(*k*). In a perfect lattice, a charge carrier with an effective mass $m^*(k) \equiv (\partial^2 E(k)/\hbar^2 \partial k^2)^{-1}$ propagates at the group velocity $v(k) \equiv \partial E(k)/\hbar \partial k$ without any scattering.[121–123] Molecules are held together in a solid by weak Van der Waals forces causing large thermal molecular motions at the room temperature and increased electron scattering.[16] Consequently, band transport theory breaks down in the presence of crystal's inherent large scatterings leading to mean-free-path smaller than intermolecular spacing, i.e. below the Mott-Ioffe-Regel (MIR) limit.[124,125]

It is expected that at higher temperatures the fluctuations and therefore scatterings become more profound. To estimate what is the maximum temperature for which the band theory can be applied, Bredas and co-workers compared the thermal-averaged velocity-velocity tensors and the experimental mobility data and reached the conclusion that the band model can be applied for temperatures only up to about 150 K, i.e. the band transport theory is inadequate for room temperature.[126] To determine the value of the mobility corresponding to the MIR condition (i.e. the lower limit of band theory), in Ref.[21], starting from the semiclassical Drude expression $\mu = \frac{et}{m^*}$ (with t being the time interval between two successive scattering events), the authors evaluated the mobility for a one-dimensional model of rubrene by taking J = 143 meV and T = 300 K. They attained MIR corresponding mobility of 23 cm^2/Vs and a similar estimation was also made in ref.[126]. Therefore, one can conclude that high-mobility molecular semiconductors at room temperature have mobilities above the (maximum) hopping limit and below the (minimum) MIR limit requiring new methods to deal with their charge transport properties (at low temperatures they may have higher mobility consistent with band transport).

The scattering of the Bloch states by the molecular vibrations can be included as a perturbation in the band transport model[127] and methods combining band theory and many-body perturbation theory are expected to accurately capture electron-phonon scattering. However, due to high computational cost, these calculations have been only applied to inorganic materials[128,129] with small unit cells but not to organic semiconductors with relatively large unit cells. There have been also other attempts to the generalization of the band transport theory e.g. by considering acoustic deformation potential model in the calculation of relaxation times of charge carriers[130–132] where the basic assumption is that the scattering originates from the acoustic phonons and their impact can be considered by a uniform lattice dilation or deformation.[133] In ref.[68], N.-E. Lee and co-workers, in the framework of ab initio band theory, have carried out DFT calculations employing a plane-wave basis set by considering the Grimme van der Waals (vdW) correction[134] in structural relaxation. Phonon dispersions are computed with density functional perturbation theory (DFPT)[135] and the electron-phonon coupling matrix elements using the EPW code.[136] It should be remembered that all these methods are expected to provide reliable results only in the limit of a relatively weak dynamic disorder, e.g. at low temperature. Moreover, the ab-initio based band models such as ref.[68] are quite computationally demanding (the work was carried out for naphthalene), well suited for benchmark studies rather than materials discovery work.

Small polaron theory. Small polaron theory describes the charge carriers alongside a dressing cloud of phonons and was introduced by Holstein to describe the impact of local electron-phonon coupling on the

charge dynamics.[78] The theory predicts that, in response to electron-phonon couplings, the charge carrier becomes increasingly more localized leading to narrower bands at increasing temperature,[93] and experiments such as ARPES which have demonstrated this effect.[137,138] The band narrowing factor can be obtained by Lang-Firsov canonical transformation of the Hamiltonian followed by thermal averaging over the phonon modes as,[139]

$$f = \exp(-\sum_{M}(g_{i,M}/\hbar\omega_{M})^{2}(2N_{M}+1)) \quad (13)$$

with $N_{M} = \left(\exp(\hbar\omega_{M}/k_{B}T)-1\right)^{-1}$ being the occupation number. In principle, band narrowing is equivalent to assuming that the transfer integrals can be replaced by "thermally averaged" transfer integrals. As the band narrowing is larger at high temperatures, the consequence of this theory is that the transport is band-like at low temperatures with the charge-carrier mobility decreasing with temperature in a power-law form[140] and a hopping like behavior at high temperatures when the bandwidth became too small to sustain delocalized states.[7,141,142]

An attempt to extend the transport theory to incorporate the impact of both local and nonlocal electron-phonon couplings was initiated by Munn and Silbey considering a Holstein-Peierls type Hamiltonian.[143,144] Unlike in the original Holstein model, which always yields a narrower band, it was found that the presence of nonlocal coupling changes the shape of the band and depending on the system's parameters may lead to band broadening. In another study, Bobbert and co-workers[93,145] fitted microscopic parameters extracted from ab initio calculations into the same type of Hamiltonian and were able to reproduce the experimental data of naphthalene crystal, even when neglecting the coupling with acoustic modes.[145] Polaron theory has the same shortcomings of the band theory, i.e. short mean free path and mobility falling below the MIR limit.

Polaronic theories still play an important role in treating the coupling between the carrier and high-frequency modes. The thermal averaging required to derive equations like (13) is justified for vibrational modes, which are faster than the carriers (larger than $\hbar/J$). However, as shown in Figure (2), the vibrational frequencies coupled with the carrier are spread out over a large window meaning that the band-narrowing picture can only be "partially" justified. Moreover, the fluctuations of the transfer integrals take place at the same timescale as the carrier and are extremely large in amplitude. This suggests that an ideal feature of any theory is the ability to describe the coupling of the electron with phonons of a broad range of energies.

Mixed quantum-classical approaches. The main motivation in developing mixed quantum-classical approaches is to provide an optimal combination of satisfactory accuracy and reasonable computational cost for the study of electron-phonon interactions.[23,146–148] These approaches assume that due to the different nature of electrons and nuclei involved in charge transport, only the former should be evaluated quantum mechanically, while the latter can be treated classically. These semi-classical approaches are usually classified into two main categories: the Mean-Field Ehrenfest (MFE) and trajectory surface hopping (TSH) which are both non-perturbative methods differing in the way they describe the classical equations of motion for the nuclei.

Mean-Field Ehrenfest model. In the MFE method, the system propagates on a potential energy surface obtained based on weighted averaging over all adiabatic states.[149,150] The implementation of the MFE in the field of charge transport was initiated by introducing the context of polaron and soliton in conductive polymers utilizing Su-Schrieffer-Heeger (SSH) model Hamiltonian.[151,152] The method was applied to molecular crystals to propose for the first time that the transport is limited by dynamic disorder and to explain the coexistence of localized states and coherent transport with band-like dependence of the mobility from the temperature.[16,153] It has sufficiently efficient scaling that could be extended to two-dimensions.[154–156] A recent work proposes an even more approximated MFE, where the charge evolves under the field of classical oscillations of the lattice unperturbed by the carrier.[157]

Due to its simplicity and straightforward implementation, MFE is widely used in different contexts,[16,102,158] but a number of weaknesses are also well documented. In particular, (i) the mean-field approximation of the back-reaction of electrons on nuclear motion can lead to the overheating of the electronic system and consequently breaks balance condition,[159] (ii) the net adiabatic character of the wavefunction cannot be recovered even in the asymptotic regions of configuration space.[160] Many of the weaknesses of MFE are particularly evident and broadly discussed in the context of chemical dynamics, with problems involving very few adiabatic states and with well-defined bonding character.[161,162] However, in solid-state problems with a continuum of electronic delocalized states it is perfectly acceptable for the wavefunction to be a superposition of electronic eigenstates (e.g. it is implicitly accepted in band transport).

Despite the great advantages of the MFE, its validity for charge transport simulations is debated. In the year 2013, Wang and Beljonne suggested that the Ehrenfest theory leads to correct diffusion tensor elements but an inaccurate temperature dependence of the carrier mobility.[146] The authors determined that the problem occurs because the theory relies on only a single potential energy surface. This assumption leads to an infinite decoherence time of the charge carrier state which does not seem to be reasonable in the localized limit of the transport mechanism. In spite of the important shortcomings of

the MFE,[163] it is still being utilized by different groups and different methods being proposed in recent years to address the problem of over-coherence. For instance, by introducing a coherence penalty functional that accounts for decoherence effects,[164,165] or by utilizing an instantaneous decoherence correction approach with energy-dependent reweighing factors to account for the decoherence and energy relaxation processes.[166,167]

Trajectory Surface Hopping method. According to the TSH method, the nuclear dynamics of the system can be described by an ensemble of non-interacting trajectories.[23,168,169] As such, each individual trajectory evolves based on the Newtonian dynamics under the influence of a single electronic state's potential energy surface. Electronic transitions are allowed and are incorporated into the nuclear dynamics by a series of hopping events. The most popular form of the TSH is the fewest switches surface hopping (FSSH) method,[170] which minimizes the number of transitions between different potential energy surfaces (PESs). According to the FSSH, only in case of non-negligible coupling between the electronic states, a transition takes place. Considering the system's wave function $|\Psi\rangle = \sum_n c_n |\varphi_n\rangle$ ($|\varphi_n\rangle$ are basis sets), one can derive the non-adiabatic coupling matrix with elements as $V_{ij}^{ad} = \left\langle \psi_i \left| \frac{d\psi_j}{dt} \right. \right\rangle$. The probability of transition between any two adiabatic PESs (*i* and *j*) can be estimated as,[170]

$$g_{ij} = -\Delta t \frac{2\mathrm{Re}(d_{ij}^* V_{ij}^{ad})}{d_{ii}} \qquad (14)$$

where $d_{ij}^* = c_i^* c_j$ denotes the charge carrier's density matrix and Δt the molecular dynamics time step. As a result of its simple formalism and relatively acceptable balance between reliability and efficiency, the FSSH method has been widely used in non-adiabatic chemical dynamics.[171–174] However, in the original formulation, some shortcomings hinder particularly the simulation of charge transport: (i) the decay of the electronic coherences between adiabatic states is not correctly described,[170] (ii) "unavoided" crossings between potential energy surfaces are not treated properly which may lead to unphysical long-range charge transfers,[175] (iii) the decoherence correction methods are speculated to lead to un-physical long-range charge transfers,[176,177] (iv) some nuclear quantum effects such as zero-point energy and tunneling that play an important role particularly at low temperatures are not considered.[178] In the last few years effective and successful solutions to problems (i)-(iii) have been developed and applied in the context of charge transport in organic semiconductors. For instance, in Ref.[179], Blumberger and co-workers have investigated the impacts of the first three aforementioned issues on the FSSH simulation of charge

transport in organic materials. To this aim, they utilized a fragment-orbital based surface hopping (FOB-SH),[180,181] a semi-empirical approach that is developed to quantify the electronic Hamiltonian and nuclear derivatives in organic crystals. In this method, the charge carrier wavefunction is expanded on the basis of singly occupied molecular orbitals of the constituting molecules, which are computed using DFT. The on-site energies of the electronic Hamiltonian are approximated with a classical force field[182] and the electronic couplings are calculated using analytic overlap method.[33] This method is similar to semiempirical approaches such as self-consistent charge density-functional tight-binding method developed by Kubar and Elstner,[183,184] with slight differences in computation of the Hamiltonian matrix elements and nuclear forces. Beljonne and co-workers, in an attempt to address the unavoided crossing problem in the FSSH method, suggested eliminating the interaction between the states which represent weak coupling in an approach named flexible surface hopping.[101] Consequently, all adiabatic states are physically close which significantly diminish the possibility of unphysical long-range charge transfer. This method can potentially resolve this issue, but the fact that critical parameters are required to ensure stability and accuracy of the simulations makes its usage challenging and implies that parameter-free techniques would be desirable. Wang et al. classified surface crossings into four general types and presented a parameter-free crossing corrected FSSH (CC-FSSH) algorithm, which is expected to deal properly with multiple surface crossings in a given time interval. They were able to investigate electron dynamics in a series of one-dimensional Holstein models.[185–187] To investigate point (iv), ref.[178] by considering a dimer of ethylene-like molecules embedded in a bath of neon atoms and through combining the surface hopping with a path-integral simulation of nuclear dynamics, suggests that the impacts of tunneling and zero-point motion are not significant for organic materials in particular at room temperature. Moreover, it has to be noted that the tunneling is not expected to be crucial for high-mobility organic semiconductors as in this case, there are no barriers to tunnel through between equilibrium geometries of neutral and charged states. On the contrary, obviously, in the low-mobility organic materials tunneling becomes important in particular at low temperature.

Other approaches have been also developed to address one or more of the original FSSH shortcomings, although they have yet to be applied in the context of charge transport. For instance, a global flux surface hopping, which is used to compute the hopping probabilities using quantum populations instead of nonadiabatic couplings.[188,189] The local diabatization approach of FSSH (LD-FSSH) proposed by Granucci and co-workers[190,191] is developed to deal with trivial crossings. In a recent review, Wang et al. have provided a comprehensive overview of the trivial crossing problem in extended systems (e.g. many-

dimensional and many-state systems).[192] The reader is also referred to refs.[23,193] for a summary of the recent progresses in the field.

Surface hopping and mean-field methods share the problem that one of their main assumptions, namely that the phonon can be treated classically, is not strictly valid because of the non-negligible role of high-frequency modes for both local and non-local coupling as detailed in section 2. In the case of surface hopping an additional common criticism is that the method cannot be derived through a rigorous set of approximations[194] and therefore it is not easy to establish when it breaks down. The two approaches behave very differently in the limits of pure hopping or pure band transport. Surface hopping methods can deal more easily with the limit of pure hopping transport (although corrections are required[195]) and becomes increasingly problematic in the case of pure band transport (because of the high-degeneracy of the electronic states). Mean-field approaches, on the contrary, can interpolate between the intermediate regime and band transport but are unable to describe hopping transport as assume an infinite decoherence time. For reasons related to the historical development of FSSH for the study of photochemical reactions, these methods are commonly implemented with molecular Hamiltonian including all nuclear degrees of freedom and potentially able to deal with non-linearity of the coupling and the anharmonicity.[196,197] Mean-field methods are more commonly used on model Hamiltonian with a reduced number of nuclear degrees of freedom (harmonic and linearly coupled with the electrons). These reduced models, thanks to the validation of the linear coupling and harmonic approximations presented in the previous section, are more accurate than originally thought and form the basis for alternative approaches to the study of quantum dynamics in molecular crystals.

Open quantum systems. Open quantum system approaches partition the electronic-vibronic dynamics into a given set of degrees of freedom namely the "system" (in this case the electronic degrees of freedom that are of interest) and a "bath" (in this case the vibrational degrees of freedom that one does not wish to consider in detail).[198,199] The state of the system is described by its reduced density matrix that allows the evaluation of all the observable within the system,

$$\underline{\underline{\rho}}_{red}(t) = Tr_{bath}[|\Psi(t)\rangle\langle\Psi(t)|] \tag{15}$$

The time evolution of $\rho_{red}(t)$ can be written as a generalized master equation as,[198,200]

$$\dot{\rho}_{red}(t) = -\frac{i}{\hbar}[\hat{H}(t),\ \rho_{red}(t)] + \int_0^t \gamma(t,j)\rho_{red}(j)dj \tag{16}$$

with $\gamma(t,j)$ being the super-operator of "memory time'' describing the impact of the bath on the system. The main obstacle in using this equation is the fact that there is no explicit method to evaluate $\gamma(t,j)$ and several approximations have been introduced to resolve this problem.[201–204]

In the context of charge transport, due to a large number of vibrational modes in molecular semiconductors (often in the order of a few hundred), the computational cost of time-evolutions is an important obstacle toward applications of these methods. As such, they are often limited to 1D models as density matrix spaces grow quadratically with the Hilbert space dimension. In addition, these methods are often applied to model reduced Hamiltonian,[205,206] although not exclusively.[203,207] Often the spectral densities utilized in these studies, which manifest the electron-phonon interaction, do not rely on precise calculations of the phonons but rather on the parametrized baths, e.g. sub-ohmic, ohmic or super-ohmic spectral density functions.[202,208,209] For instance, Yao studied the quantum dynamics utilizing the time-dependent density matrix renormalization group algorithm considering a sub-Ohmic phonon bath which gives rise to a strong non-Markovian effect.[209] Zhao and co-workers developed a non-Markovian stochastic Schrodinger equation[210] and extended it to the reciprocal (k-) space to calculate the carrier dynamics in organic semiconductors considering an Ohmic spectral density function to account for both local and nonlocal carrier-phonon interactions.[208] The mobilities computed within the framework of open quantum system methods often present power-law behavior with temperature $\mu \propto T^{-a}$. The values of a parameter are modulated by the strength of nonlocal electron-phonon couplings: in the absence of nonlocal interactions, the behavior is bandlike power-law with $a = 2.4$ which drops down to values roughly around 1 upon increasing the interactions.[208]

Quantum Monte Carlo (QMC). Quantum Monte Carlo techniques have been recently applied to the charge transport problem in organic materials.[211–213] In this method, explicit quantum dynamics of both carrier and phonon are evaluated; therefore, they are in principle at present the most exact methods to treat the charge transport. In Ref.[212], De Filippis and co-workers have considered a one-dimensional tight-binding model with nonlocal electron-phonon coupling with a single optical phonon mode (the so-called Su-Schrieffer-Heeger (SSH) method [214]) to study the charge transport properties. The idea was to provide a description of ω- dependent optical conductivity $\sigma(\omega,T)$ and mobility of an organic crystal. To this end, they computed the current-current correlation function as,

$$\Pi(z) = -i\int_0^{\infty} dt\, e^{izt} \left\langle [j(t), j(0)] \right\rangle \tag{17}$$

where $j(t)$ denotes the real-time Heisenberg representation of the current operator and $z = \omega + i\varepsilon$ with

$e > 0$. The real part of the optical conductivity (and therefore the mobility as $\mu = \mathrm{Re}\sigma(\omega \to 0^+)/e$) is related to the imaginary-time current-current correlation function, which can be recast as,

$$P(\omega) = \int_{-\infty}^{\infty} dt \, \frac{1}{\pi} \frac{\omega e^{-\omega s}}{1 - e^{\omega/T}} \mathrm{Re}\sigma(\omega) \tag{18}$$

and is solved by employing diagrammatic[215] and worldline[211] Monte Carlo methods, both yielding the same results. The optical conductivity is obtained using a small lattice of 20 sites with periodic boundary conditions. In conformity with experimental studies, this method was able to monitor a crossover from super- to sub- diffusive motion for the rubrene crystal, which takes place in the temperature interval 150-200 K. It has to be noted that, in this work, the results are fitted to a Drude-Lorentz model depicting the presence of an electronic bound state with a small radius. This has been possible because the authors assume that there is a local deformation of the crystal lattice around the charge. Accordingly, the finite frequency absorption can be related to internal degrees of freedom of such polaron rather than to thermal molecular fluctuations. Moreover, the Quantum Monte Carlo techniques for this problem are computationally demanding and they have been restricted to one-dimensional models with one phonon mode per site so far. Therefore, they may not be practical to be extended to higher-dimensions or to be used for high throughput screenings. Other similar methods, e.g. those based on the scattering theory[216] or dynamical mean-field theory[217] are expected to produce similar results but, at present, they are also developed only for one-dimensional systems.

Transient Localization Theory (TLT). The TLT is based on the observation that the dynamic disorder leads to a "transient localization" of the wavefunctions over a characteristic timescale of the fluctuation τ.[218] One can derive a quantitative model based on this observation and the Kubo formula relating the particle's mean-squared displacements (ΔX^2, ΔY^2) and the retarded current-current anticommutator correlation function $C_{+x(y)}(t)$ of the current operator $\hat{j}_{x(y)}$:[218,219]

$$C_{+x(y)}(t) = \Theta(t)\left\langle\{\hat{j}_{x(y)}(t), \hat{j}_{x(y)}(0)\}\right\rangle \tag{19}$$

where $\Theta(t)$ is the Heaviside step function and the equation is written for a two-dimensional (2D) system. This function is directly related to the mean-square displacement of the total position operator along the chosen direction,

$$\frac{d\Delta X^2(\Delta Y^2)(t)}{dt} = \frac{1}{e^2}\int_0^t C_{+x(y)}(t')dt' \tag{20}$$

with *e* being the elementary charge. The function $C_+(t)$ can be evaluated introducing the Relaxation Time Approximation (RTA), i.e. the assumption that the function can be expressed in terms of a reference system ($C_+^{ref}(t)$) from which it decays over time. The simplest possible form of RTA is $C_+(t) = C_+^{ref}(t)e^{-t/\tau}$, where the relaxation is determined by a single characteristic time capturing the timescale of the fluctuation of the electronic Hamiltonian. The reference system usually is defined as an idealized version of the organic semiconductor with only static disorder, i.e. where all the molecular displacements are frozen. This reference ensures that, in the limit of large τ, the system recovers the dynamics of a statically disordered system subject to Anderson localization.[220] It has to be noted that the correlator $C_+(t)$ is not limited to the mentioned simple expression and a generalized expression like $C_+(t) = C_+^{ref}(t)\, f(t)$ would still be fully rigorous. All quantum dynamical methods described up to that point can be used to determine a more accurate $C_+(t)$, so that TLT can be seen as the first order approximation for any quantum dynamics with a single parameter collectively representing nuclear dynamics. Also one should note that the parameter τ, despite being not very critical for the results,[221] is not necessarily identical for all molecules and in the original theory is associated with the timescale of the transfer integral fluctuations.

A practical implementation of this model, described in Ref.[222], entails the repeated diagonalization of electronic Hamiltonian with static disorder giving the squared transient localization L^2 and the mobility (proportional to it). When the method is fed with realistic Hamiltonian parameters it produces computed mobility in excellent agreement with the experiments[69,221] and, because of its rapidity, it can be used to study a larger set of hypothetical materials.

In ref.[221], a generic 2D material was defined such that each molecule is surrounded by 6 neighbors with three distinct transfer integrals J_a, J_b, J_c as illustrated in Figure 6(a). The mobility was computed for all possible combinations of transfer integrals with $J = \sqrt{J_a^2 + J_b^2 + J_c^2}$ and constant nonlocal dynamic disorder. The resulting map of mobility (a cross-section is shown in Figure 6(b); with L^2 being the average of the squared transient localization length over x and y directions) showed some expected features (e.g. one-dimensional materials have considerably lower charge mobility with a similar level of disorder) but also more unexpected characteristics. The relative sign of the transfer integrals is important such that a system with $J_a = J_b = J_c$ has much larger hole mobility than a system with transfer integrals $-J_a = J_b = J_c$. This is a manifestation of a high degree of coherence in the transport and interference effects in the charge dynamics that are not seen in pure hopping models. Another interesting feature is that the temperature dependence of the mobility, which is normally considered a good guide for the identification of the

transport mechanism, depends on the electronic structure, i.e. it cannot be used to discriminate between models or regimes of transport.

Because of the much richer and complex phenomenology in 2D, it is interesting to consider what fraction of molecular semiconductors are expected to have bands delocalized in 1, 2, or 3 dimensions. Considering the same set of molecular semiconductors of ref.[54] and evaluating only materials with at least one transfer integral larger than 0.1 eV, one finds that about 12% of the structures are 2D, that is displaying a ratio between second and first highest (non parallel) transfer integrals larger than 0.05. The set is even more limited for 3D materials which are only 0.015% of the considered database. Therefore, one can conclude that developing charge transport models working in two dimensions is both necessary and sufficient for the family of molecular semiconductors.

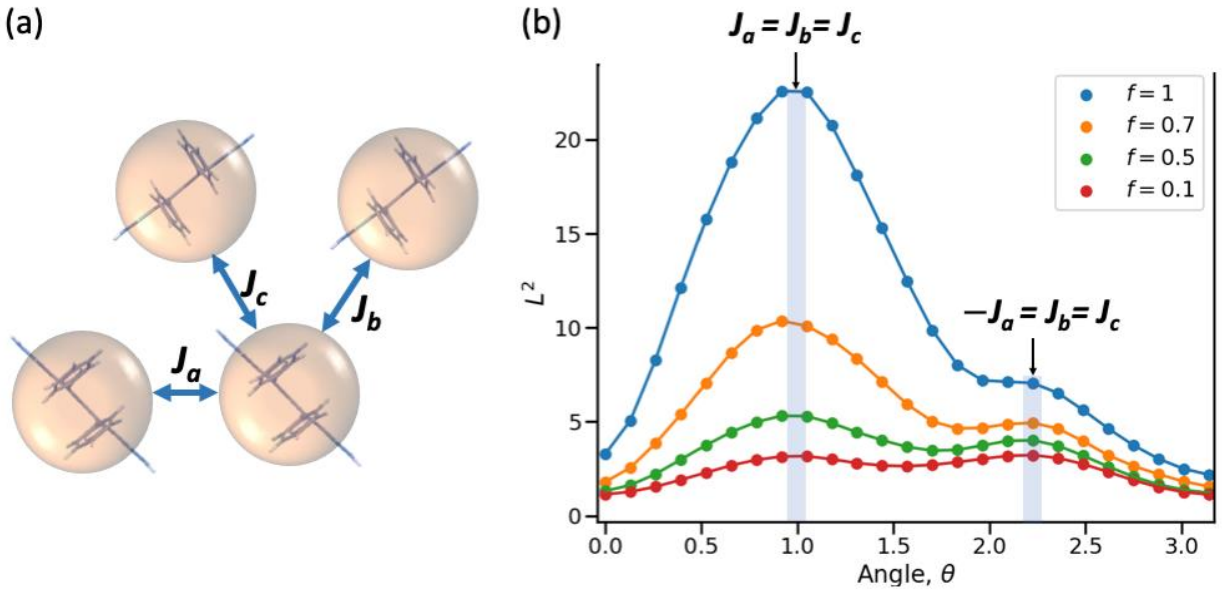

Figure 6. (a) Scheme of an idealized molecular semiconductor with electronic structure in 2D determined by the coupling with 3 neighbors (illustrated for Rubrene). (b) The squared transient localization length (proportional to the mobility) calculated at room temperature for $J_a = J\cos(q)$ and $J_b = J_c = J\sin(q)/\sqrt{2}$ with $J = 0.1$ eV, τ=0.13 ps and dynamic disorder $\frac{\sigma_a}{J_a} = \frac{\sigma_b}{J_b} = \frac{\sigma_c}{J_c} = 0.5$ (blue curve). $q = 0, p$ corresponds to a one-dimensional system with non-zero coupling only in one direction. The other curves are obtained by introducing a band renormalization factor *f*.

More recently Fratini and Ciuchi have noticed that TLT may fail for materials with reduced disorder (or at low temperature) giving way to a more straightforward band-transport mechanism with greater delocalization and rarer scattering events.[223] In the same work they have developed a unified theoretical framework which employs a correlator of the form $C(t) = C_{SC}(t) + [C_{+}^{ref}(t) - C_{SC}(t)]e^{-t/\tau}$ where $C_{SC}(t)$ denotes the correlation function in the semiclassical Boltzmann limit and the relaxation is applied only to

the correction term. The new formalism incorporates transient localization theory as a limiting case which delicately connects with the standard band transport theory.[223] The same TLT theory can also be pushed in the direction of more localized transport introducing the effect of an increasingly stronger local electron-phonon coupling. Such polaronic effects can be introduced easily in TLT if one assumes they are solely due to high-frequency modes independent from those influencing the transfer integral. In such case, their role is to scale both the transfer integral and their fluctuation by a common renormalization factor f (defined in eq. (13)). Figure 6(b), shows that, in the presence of polaronic effects, the mobility decreases (as expected) and the interference effects that made the relative sign of the coupling relevant gradually becomes less significant as one expects for pure hopping transport. It is important to note that in the case of very large reorganization energy/small band renormalization factor, the carrier becomes localized on a single molecule. In this case, the squared transient localization length L^2 is equal to the lattice spacing constant d and therefore, the theory would predict a constant (temperature and f independent) mobility of $\mu=(e/k_BT)d^2/2\tau$. It has to be noted that the theory is not strictly speaking breaking down, only the additional assumption that the characteristic time τ is a temperature independent constant would be now incorrect (the RTA would still be able to reproduce a correct mobility if fed with the correct temperature and f dependent τ); however, the advantages of the method would be completely lost.

4. Comparison with thin-film transistor measurements

As discussed in the introduction, reliable measurements of charge mobility reproducible across research groups and applicable to a broad range of materials have started appearing fairly recently.[6] An important milestone is the realization that measuring thin-film transistor mobility comparable with Hall effect mobility provides a critical proof that the observed mobility is intrinsic of the materials and not dominated by traps.[224–226] More indirect evidence of intrinsic transport is the measurement of band-like temperature dependence, i.e. mobility decreasing with increasing temperature, a phenomenology that is completely hidden if there is a considerable number of trapped charges.[227] Reference experimental data are typically obtained in single-crystals since the effect of polycrystallinity on the results is harder to quantify.[228] As a consequence of these complications, there are probably less than 20 “reference” measurements of demonstrably intrinsic mobilities in thin-film transistors that still constitute a very robust sample for the validation of the theory.[6]

Comparison of any theoretical result with a single material is useful to validate the plausibility of the theory and virtually all the theories presented in this section are able to provide mobility of the correct

order of magnitude when fed with appropriate parameters for a specific material. The comparison of the absolute value of mobility can be misleading not only because of many possible cancellations of errors in the theory but also because the experimental mobility is subject to some inaccuracy[229] and the effect of residual defects. The comparison with the temperature dependence of the mobility is less stringent than previously thought because crystal structure deformation with temperature is large enough to change the parameters of the Hamiltonian,[230] and such temperature dependence is not universal of the material class.[208,221]

Probably the best strategy to refine the current theoretical models is to compare their results for a range of materials whose mobility has been determined accurately and between different theoretical methods. This is something that several authors have started doing using surface hopping methods,[179,181] transient localization theory[69,221] and Ehrenfest propagation[231] with comparison normally extended to 5-12 materials. All these works have considered transport in two dimensions, which is essential as discussed above. Very reassuringly, these methods produce results in good agreement with each other and with the experiments[41,221] despite following different paths from the setting up of the system Hamiltonian to the computation of the mobility. A possible reason for the agreement is that the mobility is determined in all cases by the ratio between the transfer integrals and the dynamic fluctuations, which are computed with similar high accuracy in all cases.

A consequence for materials discovery is that, if one is interested in finding the "best" materials or rationalize why some materials are better, this can be done "simply" by computing the Hamiltonian parameters and a broadly similar ranking of computed mobilities can be obtained from different methods. On the other hand, if one is interested in improved transport theories, possibly covering different transport regimes, it is essential to consider more complicated experiments where the materials are perturbed in very controlled ways. Important challenges for the theory are given by the study of transport in isotopically substituted semiconductors[229,232] or materials under mechanical strain.[233–235] A recent "benchmark" experiment was proposed by the Podzorov group where Hall (intrinsic) mobility was measured while the sample was mechanically deformed.[236] Even the simple study of the temperature dependence of the mobility can be instructive, but the model should include the effect of lattice expansion which has been shown to change all parameters of the Hamiltonian in non-trivial ways.[237]

5. Conclusion

Our understanding of the theory of charge transport in molecular semiconductors underwent a very rapid acceleration in the past few years because of the contemporary improvement of the experiments (more reliable measurements on a larger set of materials), electronic structure calculations (more accessible and accurate calculations of large systems) and transport theory (a broader range of methods available). Up to very recently, it was not possible to derive any meaningful structure-property relation because the degree of confidence of the measurement, computation and theory was not sufficiently high to improve each of them independently and systematically. We showed in this perspective that each term of the Hamiltonian contributing to the mobility can be computed from first principles with a great level of confidence given by comparison with a range of more direct experimental evaluations of such terms. For the first time, it has become possible to use the comparison between computed and experimental mobility to discuss the relative merit of different theories. We have now a range of approximated theories that predict correctly the relative mobility of a set of materials and there are many opportunities to overcome the limitations of such theories by combining different aspects of each of them. For example, band renormalization can be used to account for the quantum nature of the high-frequency vibrations in all models where vibrations are treated classically and interpolation schemes can be devised to cover the parameter range between different regimes. Ideas from open quantum systems physics can be used to include the effect of low-frequency modes without explicitly describing them. Quasi exact methods on model systems provide a natural way to test more approximated theories suitable for realistic systems. The consolidation of electronic structure method and experimental measurements have created new opportunities to test novel theoretical approaches in solid-state and chemical physics.

Data availability. The data that support the findings of this study are available from the corresponding author upon reasonable request.

Acknowledgments. The authors would like to thank Alessandro Landi, Xiaoyu Xie, Daniele Padula, Simone Fratini, Sergio Ciuchi, and Adam Moule for useful discussions. This work was supported by ERC-PoC grant (Grant 403098).

References:

[1] D.D. Eley and D.I. Spivey, Trans. Faraday Soc. **57**, 2280 (1961).

[2] L.B. Schein and A.R. McGhie, Phys. Rev. B **20**, 1631 (1979).

[3] H.E. Katz, J. Mater. Chem. **7**, 369 (1997).

[4] M. Pope and C.E. Swenberg, Annu. Rev. Phys. Chem. **35**, 613 (1984).

[5] J.L. Brédas, D. Beljonne, V. Coropceanu, and J. Cornil, Chem. Rev. **104**, 4971 (2004).

[6] G. Schweicher, G. Garbay, R. Jouclas, F. Vibert, F. Devaux, and Y.H. Geerts, Adv. Mater. **32**, 1905909 (2020).

[7] T. Holstein, Ann. Phys. (N. Y). **8**, 325 (1959).

[8] T. Holstein, Ann. Phys. (N. Y). **281**, 343 (1959).

[9] A.S. Davydov, *Theory of Molecular Excitons* (Springer US, Boston, MA, 1971).

[10] H. Klauk, M. Halik, U. Zschieschang, G. Schmid, W. Radlik, and W. Weber, J. Appl. Phys. **92**, 5259 (2002).

[11] V. Podzorov, V.M. Pudalov, and M.E. Gershenson, Appl. Phys. Lett. **82**, 1739 (2003).

[12] O. Ostroverkhova, Chem. Rev. **116**, 13279 (2016).

[13] C.D. Dimitrakopoulos and P.R.L. Malenfant, Adv. Mater. **14**, 99 (2002).

[14] A.S. Alexandrov, *Polarons in Advanced Materials* (Springer Netherlands, Dordrecht, 2007).

[15] A. Troisi and G. Orlandi, J. Phys. Chem. A **110**, 4065 (2006).

[16] A. Troisi and G. Orlandi, Phys. Rev. Lett. **96**, 086601 (2006).

[17] P.M. Kazmaier and R. Hoffmann, J. Am. Chem. Soc. **116**, 9684 (1994).

[18] A. Troisi and G. Orlandi, Chem. Phys. Lett. **344**, 509 (2001).

[19] J.L. Bredas, J.P. Calbert, D.A. da Silva Filho, and J. Cornil, Proc. Natl. Acad. Sci. **99**, 5804 (2002).

[20] G. Schweicher, Y. Olivier, V. Lemaur, and Y.H. Geerts, Isr. J. Chem. **54**, 595 (2014).

[21] S. Fratini, D. Mayou, and S. Ciuchi, Adv. Funct. Mater. **26**, 2292 (2016).

[22] C. Liu, K. Huang, W.-T. Park, M. Li, T. Yang, X. Liu, L. Liang, T. Minari, and Y.-Y. Noh, Mater. Horizons **4**, 608 (2017).

[23] H. Oberhofer, K. Reuter, and J. Blumberger, Chem. Rev. **117**, 10319 (2017).

[24] P. Ordejón, D. Boskovic, M. Panhans, and F. Ortmann, Phys. Rev. B **96**, 1 (2017).

[25] Q. Wu and T. Van Voorhis, J. Chem. Phys. **125**, 164105 (2006).

[26] G. Nan and Z. Li, Sci. China Chem. **56**, 210 (2013).

[27] G. Nan, X. Yang, L. Wang, Z. Shuai, and Y. Zhao, Phys. Rev. B **79**, 115203 (2009).

[28] D.A. da Silva Filho, E.-G. Kim, and J.-L. Brédas, Adv. Mater. **17**, 1072 (2005).

[29] C. Sutton, J.S. Sears, V. Coropceanu, and J.L. Brédas, J. Phys. Chem. Lett. **4**, 919 (2013).

[30] T.P. Nguyen, J.H. Shim, and J.Y. Lee, J. Phys. Chem. C **119**, 11301 (2015).

[31] H. Kim, T. Goodson, and P.M. Zimmerman, J. Phys. Chem. Lett. **8**, 3242 (2017).

[32] A. Biancardi and M. Caricato, J. Phys. Chem. C **120**, 17939 (2016).

[33] F. Gajdos, S. Valner, F. Hoffmann, J. Spencer, M. Breuer, A. Kubas, M. Dupuis, and J. Blumberger, J. Chem. Theory Comput. **10**, 4653 (2014).

[34] Y. Kuroda, H. Ishii, S. Yoshino, and N. Kobayashi, Jpn. J. Appl. Phys. **58**, SIIB27 (2019).

[35] D. Nozaki, A. Lücke, and W.G. Schmidt, J. Phys. Chem. Lett. **8**, 727 (2017).

[36] H. Yoshida and N. Sato, Phys. Rev. B **77**, 235205 (2008).

[37] S.-H. Wen, A. Li, J. Song, W.-Q. Deng, K.-L. Han, and W.A. Goddard, J. Phys. Chem. B **113**, 8813 (2009).

[38] V. Coropceanu, J. Cornil, D.A. da Silva Filho, Y. Olivier, R. Silbey, and J.L. Brédas, Chem. Rev. **107**, 926 (2007).

[39] V. Stehr, J. Pfister, R.F. Fink, B. Engels, and C. Deibel, Phys. Rev. B **83**, 155208 (2011).

[40] S. Yin and Y. Lv, Org. Electron. **9**, 852 (2008).

[41] S. Giannini, A. Carof, M. Ellis, H. Yang, O.G. Ziogos, S. Ghosh, and J. Blumberger, Nat. Commun. **10**, 3843 (2019).

[42] M.B. Goldey, N.P. Brawand, M. Vörös, and G. Galli, J. Chem. Theory Comput. **13**, 2581 (2017).

[43] G. Nan and Z. Li, Phys. Chem. Chem. Phys. **14**, 9451 (2012).

[44] K. Niimi, S. Shinamura, I. Osaka, E. Miyazaki, and K. Takimiya, J. Am. Chem. Soc. **133**, 8732 (2011).

[45] J. Huang and M. Kertesz, Chem. Phys. Lett. **390**, 110 (2004).

[46] M.D. Newton, Chem. Rev. **91**, 767 (1991).

[47] J. Huang and M. Kertesz, J. Chem. Phys. **122**, 234707 (2005).

[48] J. Leszczynski and M.K. Shukla, *Practical Aspects of Computational Chemistry IV* (Springer US, Boston, MA, 2016).

[49] H. Ding, C. Reese, A.J. Mäkinen, Z. Bao, and Y. Gao, Appl. Phys. Lett. **96**, 222106 (2010).

[50] Y. Nakayama, Y. Uragami, S. Machida, K.R. Koswattage, D. Yoshimura, H. Setoyama, T. Okajima, K. Mase, and H. Ishii, Appl. Phys. Express **5**, 111601 (2012).

[51] J. Nitta, K. Miwa, N. Komiya, E. Annese, J. Fujii, S. Ono, and K. Sakamoto, Sci. Rep. **9**, 9645 (2019).

[52] C.R. Groom, I.J. Bruno, M.P. Lightfoot, and S.C. Ward, Acta Crystallogr. Sect. B Struct. Sci. Cryst. Eng. Mater. **72**, 171 (2016).

[53] D. Padula, Ö.H. Omar, T. Nematiaram, and A. Troisi, Energy Environ. Sci. **12**, 2412 (2019).

[54] T. Nematiaram, D. Padula, A. Landi, and A. Troisi, Adv. Funct. Mater. **DOI:** 10.1002/adfm.202001906.

[55] V. Coropceanu, R.S. Sánchez-Carrera, P. Paramonov, G.M. Day, and J.-L. Brédas, J. Phys. Chem. C **113**, 4679 (2009).

[56] X. Yang, L. Wang, C. Wang, W. Long, and Z. Shuai, Chem. Mater. **20**, 3205 (2008).

[57] V. Coropceanu, R.S. Sánchez-Carrera, P. Paramonov, G.M. Day, and J.-L. Brédas, J. Phys. Chem. C **113**, 4679 (2009).

[58] M. Abdulla, K. Refson, R.H. Friend, and P.D. Haynes, J. Phys. Condens. Matter **27**, 375402 (2015).

[59] X. Xie, A. Santana-Bonilla, and A. Troisi, J. Chem. Theory Comput. **14**, 3752 (2018).

[60] C. Schober, K. Reuter, and H. Oberhofer, J. Phys. Chem. Lett. **7**, 3973 (2016).

[61] R.G. Della Valle, E. Venuti, L. Farina, A. Brillante, M. Masino, and A. Girlando, J. Phys. Chem. B **108**, 1822 (2004).

[62] B. Aradi, B. Hourahine, and T. Frauenheim, J. Phys. Chem. A **111**, 5678 (2007).

[63] A. Landi and A. Troisi, J. Phys. Chem. C **122**, 18336 (2018).

[64] A. Brillante, I. Bilotti, R.G. Della Valle, E. Venuti, and A. Girlando, CrystEngComm **10**, 937 (2008).

[65] D. Di Nuzzo, C. Fontanesi, R. Jones, S. Allard, I. Dumsch, U. Scherf, E. von Hauff, S. Schumacher, and E. Da Como, Nat. Commun. **6**, 6460 (2015).

[66] J. Nyman, O.S. Pundyke, and G.M. Day, Phys. Chem. Chem. Phys. **18**, 15828 (2016).

[67] J.A.K. Howard, F.H. Allen, and G.P. Shields, editors , *Implications of Molecular and Materials Structure for New Technologies* (Springer Netherlands, Dordrecht, 1999).

[68] N.-E. Lee, J.-J. Zhou, L.A. Agapito, and M. Bernardi, Phys. Rev. B **97**, 115203 (2018).

[69] T.F. Harrelson, V. Dantanarayana, X. Xie, C. Koshnick, D. Nai, R. Fair, S.A. Nuñez, A.K. Thomas, T.L. Murrey, M.A. Hickner, J.K. Grey, J.E. Anthony, E.D. Gomez, A. Troisi, R. Faller, and A.J. Moulé, Mater. Horizons **6**, 182 (2019).

[70] S. Ehrlich, J. Moellmann, and S. Grimme, Acc. Chem. Res. **46**, 916 (2013).

[71] Y. Yi, V. Coropceanu, and J.L. Brédas, J. Chem. Phys. **137**, (2012).

[72] G. Schweicher, G. D'Avino, M.T. Ruggiero, D.J. Harkin, K. Broch, D. Venkateshvaran, G. Liu, A. Richard, C. Ruzié, J. Armstrong, A.R. Kennedy, K. Shankland, K. Takimiya, Y.H. Geerts, J.A. Zeitler, S. Fratini, and H. Sirringhaus, Adv. Mater. **31**, 1902407 (2019).

[73] Y. Li, V. Coropceanu, and J.L. Brédas, J. Chem. Phys. **138**, (2013).

[74] Z. Tu, Y. Yi, V. Coropceanu, and J.-L. Brédas, J. Phys. Chem. C **122**, 44 (2018).

[75] A.S. Eggeman, S. Illig, A. Troisi, H. Sirringhaus, and P.A. Midgley, Nat. Mater. **12**, 1045 (2013).

[76] S. Illig, A.S. Eggeman, A. Troisi, L. Jiang, C. Warwick, M. Nikolka, G. Schweicher, S.G. Yeates, Y. Henri Geerts, J.E. Anthony, and H. Sirringhaus, Nat. Commun. **7**, 1 (2016).

[77] G. Kresse and J. Furthmüller, Comput. Mater. Sci. **6**, 15 (1996).

[78] G. Kresse and D. Joubert, Phys. Rev. B **59**, 1758 (1999).

[79] J. Klimeš, D.R. Bowler, and A. Michaelides, Phys. Rev. B **83**, 195131 (2011).

[80] V.F. Sears, Neutron News **3**, 26 (1992).

[81] S.J. Fisher, M.P. Blakeley, E.I. Howard, I. Petit-Haertlein, M. Haertlein, A. Mitschler, A. Cousido-Siah, A.G. Salvay, A. Popov, C. Muller-Dieckmann, T. Petrova, and A. Podjarny, Acta Crystallogr. Sect. D Biol. Crystallogr. **70**, 3266 (2014).

[82] I. Natkaniec, E.L. Bokhenkov, B. Dorner, J. Kalus, G.A. Mackenzie, G.S. Pawley, U. Schmelzer, and E.F. Sheka, J. Phys. C Solid State Phys. **13**, 4265 (1980).

[83] B. Dorner, E.L. Bokhenkov, S.L. Chaplot, J. Kalus, I. Natkaniec, G.S. Pawley, U. Schmelzer, and E.F. Sheka, J. Phys. C Solid State Phys. **15**, 2353 (1982).

[84] E.A. Silinsh, A. Klimkāns, S. Larsson, and V. Čápek, Chem. Phys. **198**, 311 (1995).

[85] J.-H. Pan, Y.-M. Chou, H.-L. Chiu, and B.-C. Wang, J. Phys. Org. Chem. **20**, 743 (2007).

[86] J.E. Norton and J.-L. Brédas, J. Am. Chem. Soc. **130**, 12377 (2008).

[87] D.P. McMahon and A. Troisi, J. Phys. Chem. Lett. **1**, 941 (2010).

[88] V. Coropceanu, M. Malagoli, D.A. da Silva Filho, N.E. Gruhn, T.G. Bill, and J.L. Brédas, Phys. Rev. Lett. **89**, 275503 (2002).

[89] M. Malagoli, V. Coropceanu, D.A. da Silva Filho, and J.L. Brédas, J. Chem. Phys. **120**, 7490 (2004).

[90] F.J. Avila Ferrer and F. Santoro, Phys. Chem. Chem. Phys. **14**, 13549 (2012).

[91] M.J. Frisch, G.W. Trucks, H.B. Schlegel, and others, Gaussian Inc., Wallingford CT (2016).

[92] Z. Shuai, H. Geng, W. Xu, Y. Liao, and J.M. André, Chem. Soc. Rev. **43**, 2662 (2014).

[93] K. Hannewald, V.M. Stojanović, J.M.T. Schellekens, P.A. Bobbert, G. Kresse, and J. Hafner, Phys. Rev. B **69**, 075211 (2004).

[94] S. Kera, S. Hosoumi, K. Sato, H. Fukagawa, S. Nagamatsu, Y. Sakamoto, T. Suzuki, H. Huang, W. Chen, A.T.S. Wee, V. Coropceanu, and N. Ueno, J. Phys. Chem. C **117**, 22428 (2013).

[95] H. Yamane, S. Nagamatsu, H. Fukagawa, S. Kera, R. Friedlein, K.K. Okudaira, and N. Ueno, Phys. Rev. B **72**, 153412 (2005).

[96] F. Giustino, Rev. Mod. Phys. **89**, 015003 (2017).

[97] R.S. Sánchez-Carrera, P. Paramonov, G.M. Day, V. Coropceanu, and J.-L. Brédas, J. Am. Chem. Soc. **132**, 14437 (2010).

[98] T. Vehoff, Y.S. Chung, K. Johnston, A. Troisi, D.Y. Yoon, and D. Andrienko, J. Phys. Chem. C **114**, 10592 (2010).

[99] L. Wang, Q. Li, Z. Shuai, L. Chen, and Q. Shi, Phys. Chem. Chem. Phys. **12**, 3309 (2010).

[100] H. Oberhofer and J. Blumberger, Phys. Chem. Chem. Phys. **14**, 13846 (2012).

[101] L. Wang and D. Beljonne, J. Phys. Chem. Lett. **4**, 1888 (2013).

[102] A. Heck, J.J. Kranz, T. Kubař, and M. Elstner, J. Chem. Theory Comput. **11**, 5068 (2015).

[103] A. Troisi, Org. Electron. **12**, 1988 (2011).

[104] Z. Shuai, L. Wang, and Q. Li, Adv. Mater. **23**, 1145 (2011).

[105] P.D. Kolokathis and D.N. Theodorou, J. Chem. Phys. **137**, 034112 (2012).

[106] W.Q. Deng and W.A. Goddard, J. Phys. Chem. B **108**, 8614 (2004).

[107] B. Baumeier, J. Kirkpatrick, and D. Andrienko, Phys. Chem. Chem. Phys. **12**, 11103 (2010).

[108] W.-Q. Deng and W.A. Goddard, J. Phys. Chem. B **108**, 8614 (2004).

[109] R.A. Marcus, Angew. Chemie Int. Ed. English **32**, 1111 (1993).

[110] T. Holstein, Philos. Mag. B **37**, 499 (1978).

[111] L. Landau, *Collected Papers of L.D. Landau* (Elsevier, 1965).

[112] C. Zener, Proc. R. Soc. London. Ser. A, Contain. Pap. a Math. Phys. Character **137**, 696 (1932).

[113] M. Newton, Annu. Rev. Phys. Chem. **35**, 437 (1984).

[114] N.S. Hush, Coord. Chem. Rev. **64**, 135 (1985).

[115] J. Spencer, L. Scalfi, A. Carof, and J. Blumberger, Faraday Discuss. **195**, 215 (2016).

[116] Y. ZHAO and H. NAKAMURA, J. Theor. Comput. Chem. **05**, 299 (2006).

[117] J. Jortner, J. Chem. Phys. **64**, 4860 (1976).

[118] Y. Jiang, H. Geng, W. Shi, Q. Peng, X. Zheng, and Z. Shuai, J. Phys. Chem. Lett. **5**, 2267 (2014).

[119] A. Landi, R. Borrelli, A. Capobianco, A. Velardo, and A. Peluso, J. Phys. Chem. C **122**, 25849 (2018).

[120] Y. Yan, M. Xu, Y. Liu, and Q. Shi, J. Chem. Phys. **150**, 234101 (2019).

[121] S.H. Glarum, J. Phys. Chem. Solids **24**, 1577 (1963).

[122] L.B. Schein, C.B. Duke, and A.R. McGhie, Phys. Rev. Lett. **40**, 197 (1978).

[123] O.H. LeBlanc, J. Chem. Phys. **35**, 1275 (1961).

[124] N.G. Martinelli, Y. Olivier, S. Athanasopoulos, M.-C. Ruiz Delgado, K.R. Pigg, D.A. da Silva Filho, R.S. Sánchez-Carrera, E. Venuti, R.G. Della Valle, J.-L. Brédas, D. Beljonne, and J. Cornil, ChemPhysChem **10**, 2265 (2009).

[125] M.E. Gershenson, V. Podzorov, and A.F. Morpurgo, Rev. Mod. Phys. **78**, 973 (2006).

[126] Y.C. Cheng, R.J. Silbey, D.A. Da Silva Filho, J.P. Calbert, J. Cornil, and J.L. Brédas, J. Chem. Phys. **118**, 3764 (2003).

[127] L. Friedman, Phys. Rev. **140**, A1649 (1965).

[128] J.I. Mustafa, M. Bernardi, J.B. Neaton, and S.G. Louie, Phys. Rev. B **94**, 155105 (2016).

[129] J.-J. Zhou and M. Bernardi, Phys. Rev. B **94**, 201201 (2016).

[130] L. Tang, M. Long, D. Wang, and Z. Shuai, Sci. China Ser. B Chem. **52**, 1646 (2009).

[131] H. Kobayashi, N. Kobayashi, S. Hosoi, N. Koshitani, D. Murakami, R. Shirasawa, Y. Kudo, D. Hobara, Y. Tokita, and M. Itabashi, J. Chem. Phys. **139**, 014707 (2013).

[132] J.E. Northrup, Appl. Phys. Lett. **99**, 062111 (2011).

[133] Z. Shuai, L. Wang, and C. Song, *Theory of Charge Transport in Carbon Electronic Materials* (Springer Berlin Heidelberg, Berlin, Heidelberg, 2012).

[134] S. Grimme, J. Comput. Chem. **27**, 1787 (2006).

[135] S. Baroni, S. de Gironcoli, A. Dal Corso, and P. Giannozzi, Rev. Mod. Phys. **73**, 515 (2001).

[136] S. Poncé, E.R. Margine, C. Verdi, and F. Giustino, Comput. Phys. Commun. **209**, 116 (2016).

[137] N. Koch, A. Vollmer, I. Salzmann, B. Nickel, H. Weiss, and J.P. Rabe, Phys. Rev. Lett. **96**, 156803 (2006).

[138] Y. Nakayama, Y. Mizuno, M. Hikasa, M. Yamamoto, M. Matsunami, S. Ideta, K. Tanaka, H. Ishii, and N. Ueno, J. Phys. Chem. Lett. **8**, 1259 (2017).

[139] I. Lang and Y. Firsov, Sov. J. Exp. Theor. Phys. **16**, 1301 (1963).

[140] C. Motta and S. Sanvito, J. Chem. Theory Comput. **10**, 4624 (2014).

[141] D. Chen, J. Ye, H. Zhang, and Y. Zhao, J. Phys. Chem. B **115**, 5312 (2011).

[142] V. Coropceanu, J. Cornil, D.A. da Silva Filho, Y. Olivier, R. Silbey, and J.-L. Brédas, Chem. Rev. **107**, 926 (2007).

[143] R.W. Munn and R. Silbey, J. Chem. Phys. **83**, 1843 (1985).

[144] R.W. Munn and R. Silbey, J. Chem. Phys. **83**, 1854 (1985).

[145] K. Hannewald and P.A. Bobbert, Appl. Phys. Lett. **85**, 1535 (2004).

[146] L. Wang and D. Beljonne, J. Chem. Phys. **139**, 064316 (2013).

[147] A. V. Akimov, A.J. Neukirch, and O. V. Prezhdo, Chem. Rev. **113**, 4496 (2013).

[148] W. Xie, D. Holub, T. Kubař, and M. Elstner, J. Chem. Theory Comput. **16**, 2071 (2020).

[149] J.B. Delos, W.R. Thorson, and S.K. Knudson, Phys. Rev. A **6**, 709 (1972).

[150] G.D. Billing, Int. Rev. Phys. Chem. **13**, 309 (1994).

[151] W.P. Su, J.R. Schrieffer, and A.J. Heeger, Phys. Rev. Lett. **42**, 1698 (1979).

[152] A.A. Johansson and S. Stafström, Phys. Rev. B **69**, 235205 (2004).

[153] M. Hultell and S. Stafström, Chem. Phys. Lett. **428**, 446 (2006).

[154] S. Stafström, Chem. Soc. Rev. **39**, 2484 (2010).

[155] A. Troisi, J. Chem. Phys. **134**, (2011).

[156] E. Mozafari and S. Stafström, J. Chem. Phys. **138**, 184104 (2013).

[157] H. Ishii, J. Inoue, N. Kobayashi, and K. Hirose, Phys. Rev. B **98**, 235422 (2018).

[158] J. le Page, D.R. Mason, and W.M.C. Foulkes, J. Phys. Condens. Matter **20**, 125212 (2008).

[159] M. Barbatti, Wiley Interdiscip. Rev. Comput. Mol. Sci. **1**, 620 (2011).

[160] M.D. Hack and D.G. Truhlar, J. Chem. Phys. **114**, 2894 (2001).

[161] M. Barbatti, Wiley Interdiscip. Rev. Comput. Mol. Sci. **1**, 620 (2011).

[162] J.C. Tully, J. Chem. Phys. **137**, 22A301 (2012).

[163] L. Wang, D. Beljonne, L. Chen, and Q. Shi, J. Chem. Phys. **134**, 244116 (2011).

[164] A. V. Akimov, R. Long, and O. V. Prezhdo, J. Chem. Phys. **140**, 194107 (2014).

[165] P. Nijjar, J. Jankowska, and O. V. Prezhdo, J. Chem. Phys. **150**, 204124 (2019).

[166] W. Si and C.Q. Wu, J. Chem. Phys. **143**, (2015).

[167] J. Dong, W. Si, and C.-Q. Wu, J. Chem. Phys. **144**, 144905 (2016).

[168] O. V. Prezhdo and P.J. Rossky, J. Chem. Phys. **107**, 5863 (1997).

[169] J.E. Subotnik, A. Jain, B. Landry, A. Petit, W. Ouyang, and N. Bellonzi, Annu. Rev. Phys. Chem. **67**, 387 (2016).

[170] J.C. Tully, J. Chem. Phys. **93**, 1061 (1990).

[171] C. Ciminelli, G. Granucci, and M. Persico, Chem. - A Eur. J. **10**, 2327 (2004).

[172] S. Hammes-Schiffer, Acc. Chem. Res. **39**, 93 (2006).

[173] M. Barbatti and R. Crespo-Otero, in *Pept. Mater.* (2014), pp. 415–444.

[174] L. Wang, R. Long, and O. V. Prezhdo, Annu. Rev. Phys. Chem. **66**, 549 (2015).

[175] L. Wang and O. V. Prezhdo, J. Phys. Chem. Lett. **5**, 713 (2014).

[176] X. Bai, J. Qiu, and L. Wang, J. Chem. Phys. **148**, 104106 (2018).

[177] S. Giannini, A. Carof, and J. Blumberger, J. Phys. Chem. Lett. **9**, 3116 (2018).

[178] S. Ghosh, S. Giannini, K. Lively, and J. Blumberger, Faraday Discuss. **221**, 501 (2020).

[179] A. Carof, S. Giannini, and J. Blumberger, Phys. Chem. Chem. Phys. **21**, 26368 (2019).

[180] A. Carof, S. Giannini, and J. Blumberger, J. Chem. Phys. **147**, 214113 (2017).

[181] J. Spencer, F. Gajdos, and J. Blumberger, J. Chem. Phys. **145**, (2016).

[182] D.A. Case, T.A. Darden, I. T.E. Cheatham, C.L. Simmerling, J. Wang, R.E. Duke, R. Luo, M. Crowley, R.C. Walker, W. Zhang, K.M. Merz, B.Wang, S. Hayik, A. Roitberg, G. Seabra, I. Kolossváry, K.F.Wong, F. Paesani, J. Vanicek, X.Wu, S.R. Brozell, T. Steinbrecher, H. Gohlke, L. Yang, C. Tan, J. Mongan, V. Hornak, G. Cui, D.H. Mathews, M.G. Seetin, C. Sagui, V. Babin, and P.A. Kollman, Univ. California, San Fr. 1 (2008).

[183] T. Kubař and M. Elstner, J. R. Soc. Interface **10**, 20130415 (2013).

[184] T. Kubař and M. Elstner, Phys. Chem. Chem. Phys. **15**, 5794 (2013).

[185] L.J. Wang, Q. Peng, Q.K. Li, and Z. Shuai, J. Chem. Phys. **127**, 044506 (2007).

[186] L.J. Wang, Q.K. Li, and Z. Shuai, J. Chem. Phys. **128**, 194706 (2008).

[187] J. Qiu, X. Bai, and L. Wang, J. Phys. Chem. Lett. **9**, 4319 (2018).

[188] L. Wang, D. Trivedi, and O. V. Prezhdo, J. Chem. Theory Comput. **10**, 3598 (2014).

[189] A.E. Sifain, L. Wang, and O. V. Prezhdo, J. Chem. Phys. **142**, 224102 (2015).

[190] G. Granucci, M. Persico, and A. Toniolo, J. Chem. Phys. **114**, 10608 (2001).

[191] F. Plasser, G. Granucci, J. Pittner, M. Barbatti, M. Persico, and H. Lischka, J. Chem. Phys. **137**, 22A514 (2012).

[192] L. Wang, J. Qiu, X. Bai, and J. Xu, WIREs Comput. Mol. Sci. **10**, 1 (2020).

[193] L. Wang, A. Akimov, and O. V. Prezhdo, J. Phys. Chem. Lett. **7**, 2100 (2016).

[194] S.C. Althorpe, W. Barford, J. Blumberger, C. Bungey, I. Burghardt, A. Datta, S. Ghosh, S. Giannini, T. Grünbaum, S. Habershon, S. Hammes-Schiffer, S. Hay, S. Iyengar, G. Jones, A. Kelly, K. Komarova, J. Lawrence, Y. Litman, J. Mannouch, D. Manolopoulos, C. Martens, R.J. Maurer, M. Melander, M. Rossi, K. Sakaushi, M. Saller, A. Schile, S. Sturniolo, G. Trenins, and G. Worth, Faraday Discuss. **221**, 564 (2020).

[195] M.J. Falk, B.R. Landry, and J.E. Subotnik, J. Phys. Chem. B **118**, 8108 (2014).

[196] A.A. Kananenka, C.-Y. Hsieh, J. Cao, and E. Geva, J. Phys. Chem. Lett. **9**, 319 (2018).

[197] A.S. Petit and J.E. Subotnik, J. Chem. Phys. **141**, 014107 (2014).

[198] S. Nakajima, Prog. Theor. Phys. **20**, 948 (1958).

[199] V. May and O. Kühn, *Charge and Energy Transfer Dynamics in Molecular Systems* (Wiley-VCH Verlag GmbH & Co. KGaA, Weinheim, Germany, 2011).

[200] R. Zwanzig, J. Chem. Phys. **33**, 1338 (1960).

[201] G.S. Agarwal, Zeitschrift Für Phys. A Hadron. Nucl. **258**, 409 (1973).

[202] A. Pereverzev and E.R. Bittner, J. Chem. Phys. **125**, 104906 (2006).

[203] F.A.Y.N. Schröder, D.H.P. Turban, A.J. Musser, N.D.M. Hine, and A.W. Chin, Nat. Commun. **10**, 1062 (2019).

[204] J. Gambetta and H.M. Wiseman, Phys. Rev. A **66**, 052105 (2002).

[205] J. Roden, W.T. Strunz, K.B. Whaley, and A. Eisfeld, J. Chem. Phys. **137**, 204110 (2012).

[206] D. Xu and J. Cao, Front. Phys. **11**, 110308 (2016).

[207] A.M. Alvertis, F.A.Y.N. Schröder, and A.W. Chin, J. Chem. Phys. **151**, 084104 (2019).

[208] M. Lian, Y.-C. Wang, Y. Ke, and Y. Zhao, J. Chem. Phys. **151**, 044115 (2019).

[209] Y. Yao, New J. Phys. **19**, (2017).

[210] Y. Ke and Y. Zhao, J. Chem. Phys. **147**, 184103 (2017).

[211] A.S. Mishchenko, N. Nagaosa, G. De Filippis, A. de Candia, and V. Cataudella, Phys. Rev. Lett. **114**, 146401 (2015).

[212] G. De Filippis, V. Cataudella, A.S. Mishchenko, N. Nagaosa, A. Fierro, and A. De Candia, Phys. Rev. Lett. **114**, 1 (2015).

[213] A. de Candia, G. De Filippis, L.M. Cangemi, A.S. Mishchenko, N. Nagaosa, and V. Cataudella, EPL (Europhysics Lett. **125**, 47002 (2019).

[214] D.J.J. Marchand, G. De Filippis, V. Cataudella, M. Berciu, N. Nagaosa, N. V. Prokof'ev, A.S. Mishchenko, and P.C.E. Stamp, Phys. Rev. Lett. **105**, 266605 (2010).

[215] N. V. Prokof'ev and B. V. Svistunov, Phys. Rev. Lett. **81**, 2514 (1998).

[216] T. Nematiaram, A. Asgari, and D. Mayou, J. Chem. Phys. **152**, 044109 (2020).

[217] K.-D. Richler and D. Mayou, Phys. Rev. B **99**, 195151 (2019).

[218] S. Ciuchi, S. Fratini, and D. Mayou, Phys. Rev. B **83**, 081202 (2011).

[219] S. Fratini, S. Ciuchi, and D. Mayou, Phys. Rev. B **89**, 235201 (2014).

[220] P.W. Anderson, Rev. Mod. Phys. **50**, 191 (1978).

[221] S. Fratini, S. Ciuchi, D. Mayou, G.T. de Laissardière, and A. Troisi, Nat. Mater. **16**, 998 (2017).

[222] T. Nematiaram, S. Ciuchi, X. Xie, S. Fratini, and A. Troisi, J. Phys. Chem. C **123**, 6989 (2019).

[223] S. Fratini and S. Ciuchi, Phys. Rev. Res. **2**, 013001 (2020).

[224] V. Podzorov, E. Menard, J.A. Rogers, and M.E. Gershenson, Phys. Rev. Lett. **95**, 226601 (2005).

[225] H.T. Yi, Y.N. Gartstein, and V. Podzorov, Sci. Rep. **6**, 23650 (2016).

[226] J.-F. Chang, T. Sakanoue, Y. Olivier, T. Uemura, M.-B. Dufourg-Madec, S.G. Yeates, J. Cornil, J. Takeya, A. Troisi, and H. Sirringhaus, Phys. Rev. Lett. **107**, 066601 (2011).

[227] Y. Mei, P.J. Diemer, M.R. Niazi, R.K. Hallani, K. Jarolimek, C.S. Day, C. Risko, J.E. Anthony, A. Amassian, and O.D. Jurchescu, Proc. Natl. Acad. Sci. **114**, E6739 (2017).

[228] I. Vladimirov, M. Kühn, T. Geßner, F. May, and R.T. Weitz, Sci. Rep. **8**, 14868 (2018).

[229] X. Ren, M.J. Bruzek, D.A. Hanifi, A. Schulzetenberg, Y. Wu, C.-H. Kim, Z. Zhang, J.E. Johns, A. Salleo, S. Fratini, A. Troisi, C.J. Douglas, and C.D. Frisbie, Adv. Electron. Mater. **3**, 1700018 (2017).

[230] Y. Li, V. Coropceanu, and J.-L. Brédas, J. Phys. Chem. Lett. **3**, 3325 (2012).

[231] H. Tamura, M. Tsukada, H. Ishii, N. Kobayashi, and K. Hirose, Phys. Rev. B **86**, 035208 (2012).

[232] W. Xie, K.A. McGarry, F. Liu, Y. Wu, P.P. Ruden, C.J. Douglas, and C.D. Frisbie, J. Phys. Chem. C **117**, 11522 (2013).

[233] M. Matta, M.J. Pereira, S.M. Gali, D. Thuau, Y. Olivier, A. Briseno, I. Dufour, C. Ayela, G. Wantz, and L.

Muccioli, Mater. Horizons **5**, 41 (2018).

[234] M.T. Ruggiero, S. Ciuchi, S. Fratini, and G. D'Avino, J. Phys. Chem. C **123**, 15897 (2019).

[235] T. Kubo, R. Häusermann, J. Tsurumi, J. Soeda, Y. Okada, Y. Yamashita, N. Akamatsu, A. Shishido, C. Mitsui, T. Okamoto, S. Yanagisawa, H. Matsui, and J. Takeya, Nat. Commun. **7**, (2016).

[236] H.H. Choi, H.T. Yi, J. Tsurumi, J.J. Kim, A.L. Briseno, S. Watanabe, J. Takeya, K. Cho, and V. Podzorov, Adv. Sci. **7**, 1901824 (2020).

[237] A. Landi, A. Troisi, and A. Peluso, J. Mater. Chem. C **7**, 9665 (2019).